Geochemistry Geophysics Geosystems G3
AN ELECTRONIC JOURNAL OF THE EARTH SCIENCES
Published by AGU and the Geochemical Society

Article
Volume 5, Number 9
10 September 2004
Q09F26, doi:10.1029/2004GC000744
ISSN: 1525-2027

Seawater-peridotite interactions: First insights from ODP Leg 209, MAR 15°N

Wolfgang Bach
Department of Marine Chemistry and Geochemistry, Woods Hole Oceanographic Institution, 360 Woods Hole Road, MS #8, Woods Hole, Massachusetts 02543, USA (wbach@whoi.edu)

Carlos J. Garrido
Departamento de Mineralogia y Petrologia, Facultad de Ciencias, Universidad de Granada, Fuentenuva s/n, 18002 Granada, Spain

Holger Paulick
Mineralogisch-petrologisches Institut, Universität Bonn, Poppelsdorfer Schloss, Bonn 53115, Germany

Jason Harvey
Department of Earth Sciences, The Open University, Walton Hall, Milton Keynes MK7 6AA, UK

Martin Rosner
Department of Inorganic and Isotope Geochemistry, GeoForschungsZentrum Potsdam, Telegrafenberg B122, 14473 Potsdam, Germany

[1] We present first results of a petrographic study of hydrothermally altered peridotites drilled during Ocean Drilling Program (ODP) Leg 209 in the 15°20′N fracture Zone area on the Mid-Atlantic Ridge (MAR). We find that serpentinization is extensive at all drill sites. Where serpentinization is incomplete, phase relations indicate two major reaction pathways. One is reaction of pyroxene to talc and tremolite, and the other is reaction of olivine to serpentine, magnetite, and brucite. We interpret these reactions in the light of recent peridotite-seawater reaction experiments and compositions of fluids venting from peridotite massifs at a range of temperatures. We suggest that the replacement of pyroxene by talc and tremolite takes place at temperatures >350°–400°C, where olivine is stable. The breakdown of olivine to serpentine, magnetite, and brucite is favored at temperatures below 250°C, where olivine reacts faster then pyroxene. High-temperature hydrothermal fluids venting at the Logatchev and Rainbow sites are consistent with rapid reaction of pyroxene and little or no reaction of olivine. Moderate-temperature fluids venting at the Lost City site are consistent with ongoing reaction of olivine to serpentine and brucite. Many completely serpentinized peridotites lack brucite and talc because once the more rapidly reacting phase is exhausted, interaction with the residual phase will change fluid pH and silica activity such that brucite or talc react to serpentine. At two sites we see strong evidence for continued fluid flow and fluid-rock interaction after serpentinization was complete. At Site 1268, serpentinites underwent massive replacement by talc under static conditions. This reaction requires either removal of Mg from or addition of Si to the system. We propose that the talc-altered rocks are Si-metasomatized and that the source of Si is likely gabbro-seawater reaction or breakdown of pyroxene deeper in the basement. The basement at Site 1268 is heavily veined, with talc and talc-oxide-sulfide veins being the most common vein types. It appears that the systems evolved from reducing (oxygen fugacity buffered by magnetite-pyrrhotite-pyrite and lower) to oxidizing (dominantly hematite). We propose that this transition is indicative of high fluid flux under retrograde conditions and that the abundance of hematite may relate to the Ca-depleted nature of the basement that prevents near-quantitative removal of seawater sulfate by anhydrite precipitation. At site 1272 we find abundant iowaite partly replacing brucite. While this is the first report of iowaite from a mid-ocean ridge

setting, its presence indicates, again, fairly oxidizing conditions. Our preliminary results indicate that peridotite-seawater and serpentinite-seawater interactions can take place under a wider range of temperature and redox conditions than previously appreciated.

Components: 13,445 words, 7 figures, 1 table.

Keywords: hydrothermal system; Ocean Drilling Program; oceanic crust; serpentinite; water-rock interaction.

Index Terms: 3015 Marine Geology and Geophysics: Heat flow (benthic) and hydrothermal processes; 3035 Marine Geology and Geophysics: Midocean ridge processes; 8135 Tectonophysics: Hydrothermal systems (8424).

Received 14 April 2004; **Revised** 8 July 2004; **Accepted** 28 July 2004; **Published** 10 September 2004.

Bach, W., C. J. Garrido, H. Paulick, J. Harvey, and M. Rosner (2004), Seawater-peridotite interactions: First insights from ODP Leg 209, MAR 15°N, *Geochem. Geophys. Geosyst.*, *5*, Q09F26, doi:10.1029/2004GC000744.

Theme: The Oman Ophiolite and Mid-Ocean Ridge Processes
Guest Editors: Peter Kelemen, Chris MacLeod, and Susumu Umino

1. Introduction

[2] Serpentinization of peridotites at slow-spreading mid-ocean ridges has important consequences for the rheology of oceanic lithosphere [*Escartín et al.*, 1997], geochemical budgets of the oceans [*Thompson and Melson*, 1970; *Snow and Dick*, 1995], and microbial processes within, at, and above the seafloor [*Kelley et al.*, 2001; *Holm and Charlou*, 2001; *O'Brien et al.*, 1998; *Alt and Shanks*, 1998]. Serpentinization is also believed to play an important role in setting ocean chemistry and redox conditions at the surface of planetary bodies such as Europa [*Zolotov and Shock*, 2003]. Mid-water light back-scatter and chemical anomalies along mid-ocean ridge segments that have thin or no igneous crust suggest that serpentinization and peridotite-hosted hydrothermal systems in these settings may be widespread [*German et al.*, 1998; *Bach et al.*, 2002; *Edmonds et al.*, 2003].

[3] Insights into serpentinization reactions are based on analyses of vent fluids from peridotite-hosted hydrothermal systems [*Kelley et al.*, 2001; *Charlou et al.*, 2002; *Douville et al.*, 2002], experimental and theoretical considerations [*Allen and Seyfried*, 2003], and petrographic studies (see *Mével* [2003] for a review). Experimental studies have demonstrated that pyroxenes react faster than olivine at temperatures above 250°–300°C, while olivine reacts faster than pyroxene at temperatures <250°C [*Martin and Fyfe*, 1970; *Janecky and Seyfried*, 1986; *Allen and Seyfried*, 2003]. Pyroxenes react to form serpentine, talc, and tremolite, releasing Ca, Si, H_2, and acidity to the reacting fluids that may cause rodingitization in adjacent gabbro bodies. Hydrogen may react with dissolved bicarbonate to form hydrocarbons [*Kelley and Früh-Green*, 1999, 2000; *Holm and Charlou*, 2001]. Fe-Ni-O-S phase relationships [*Craig*, 1973; *Eckstrand*, 1975; *Frost*, 1985; *Alt and Shanks*, 1998, 2003] confirm high aqueous H_2 activities in serpentinization systems. Abiotic synthesis of high-molecular weight organic compounds in these environments has been proposed [*Holm and Charlou*, 2001]; however, an abiotic nature of these components has been questioned [*Simoneit et al.*, 2004], and reaction conditions and pathways of hydrothermal organic synthesis are poorly understood [*McCollom and Seewald*, 2001].

[4] Ocean Drilling Program (ODP Leg 209 drilled mantle peridotite and gabbroic rocks along the Mid-Atlantic Ridge (MAR) between 14°N and 16°N to study along-axis variations in deformation, melt migration, and hydrothermal alteration. The recovered peridotites show a remarkable variability of serpentinization reactions and intensities of alteration including incipient serpentinization of olivine along with talc-tremolite alteration of pyroxenes, complete alteration of peridotites to serpentine and magnetite followed by replacement of serpentine by talc, various degrees of serpentine-brucite alteration, and replacement of brucite by iowaite. These rocks provide a unique opportunity to gain new insights into serpentinization reactions. Our field observations can be calibrated against recent results from experimental and theoretical geochemical and

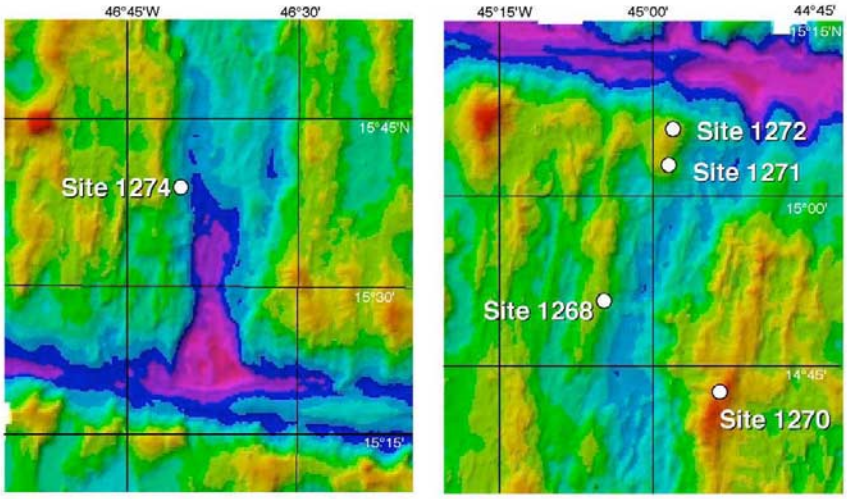

Figure 1. Location map of selected ODP Leg 209 drill sites.

petrological studies to further our understanding of serpentinization and its role in tectonic accreting and microbial colonizing of oceanic lithosphere at slow spreading ridges. We here report initial petrographic observations and discuss their bearings on mineral-fluid reactions. Detailed examinations of the timing of alteration and its relation to deformation will be presented in forthcoming communications.

2. Geological Setting and Drill Site Descriptions

[5] The area near the 15°20′N Fracture Zone (FZ) on the Mid-Atlantic Ridge (MAR) has been the focus of numerous geophysical, dredging, and submersible surveys [e.g., *Escartín and Cannat*, 1999; *Escartín et al.*, 2003; *Cannat et al.*, 1997; *Casey et al.*, 1998; *Fujiwara et al.*, 2003; *Bougault et al.*, 1988] (Figure 1). Both flanks of the MAR in the 15°20′N FZ area are composed of serpentinized mantle and gabbroic rocks, indicative of extensive crustal thinning and formation of oceanic core complexes along long-lived low-angle faults. Basaltic volcanism is scarce north of the 14°N region that is characterized by enriched-type mid-ocean ridge basalt (MORB) [*Dosso and Bougault*, 1986; *Dosso et al.*, 1993]. Mantle peridotites from 15°05′N also display enriched geochemical signatures [*Dick and Kelemen*, 1992]. The magmatic center at 14°N coincides with a large, concentric negative mantle Bouguer gravity anomaly. While a similar, but smaller, anomaly has been observed at 16°N the region in between these two gravity bullseyes shows relative gravity highs consistent with the predominance of mantle rocks at the seafloor [e.g., *Cannat et al.*, 1997; *Escartín and Cannat*, 1999; *Fujiwara et al.*, 2003]. The Logatchev hydrothermal field is located at ~14°45′N on the eastern median valley wall within steeply faulted blocks of serpentinized peridotites [*Krasnov et al.*, 1995]. Active hydrothermal venting is common in the area, as indicated by abundant and strong methane anomalies in the water column [*Bougault et al.*, 1993; *Charlou et al.*, 1998; *Sudarikov and Roumiantsev*, 2000].

[6] The following drill site description is not comprehensive, and we refer to *Shipboard Scientific Party* [2003] for details. An overview of the drilling achievements and site lithologies is provided in Table 1.

[7] Site 1268 is located on the western flank of the rift valley in flat terrain upslope and west of a steep scarp that exposes dunite and peridotite with gabbroic dikes (Figure 1). Hole 1268A penetrated 147.6 m into basement and recovered 78.7 m of core. All holes of Site 1270 spud into striated outcrops of peridotite and gabbro on the eastern flank of the MAR from 1951 to 1822 meters below sea level (mbsl). Poor recovery and the presence of fault gouge at 15–20 mbsf in every hole indicate that brittle fault zones run parallel to the fault surface that is exposed on the rift wall. This fault zone caused borehole instabilities that inhibited deep basement penetration. Site 1271 is located on the western flank of the Mid-Atlantic rift valley at a depth of about 3600 mbsl (Figure 1). Hole 1271A spudded into a smooth, sedimented slope, encountered a near-surface fault zone at around 20 mbsf and had to be abandoned after drilling

Table 1. Summary of Drill Holes With Dominantly Ultramafic Rocks

Holes	1268A	1270A	1270C	1270D	1271A	1271B	1272A	1274A
Latitude	14°50.755′N	14°43.342′N	14°43.284′N	14°43.270′N	15°02.222′N	15°02.189′N	15°05.666′N	15°38.867′N
Longitude	45°04.641W	44°53.321′W	44°53.091′W	44°53.084′W	44°56.887′W	44°56.912′W	44°58.300′W	46°40.582′W
Water depth, m	3007	1951	1822	1817	3612	3585	2560	3940
Basement penetration, m	147.6	26.9	18.6	57.3	44.8	103.6	131.0	155.8
Core recovered, m	78.7	3.3	2.0	7.7	5.8	15.9	37.5	34.7
Lithology, %								
Harzburgite	63	89	81	91	1	9	93	71
Dunite	11	5	17	7	98	56	3.5	19
Gabbroic	26	4	1	2	1	35	3.5	3
Fault gouge	-	2	1	-	-	-	-	7
Alteration of peridotite	serpentine, talc, pyrite, hematite, magnetite	serpentine, magnetite	serpentine, magnetite	serpentine, magnetite	serpentine, brucite, magnetite	serpentine, brucite, magnetite	serpentine, iowaite, brucite, aragonite	serpentine, brucite, magnetite
Alteration intensity, %	98–100	98–100	98–100	50–100	30–100	30–100	90–100	30–100%
Veining	talc, serpentine, sulfide, oxide	serpentine, talc, magnetite	serpentine, oxide, talc, carbonate	serpentine, oxide, calc, carbonate, sulfide, magnetite	serpentine, talc, amphibole, magnetite, carbonate	serpentine, magnetite, talc, carbonate, amphibole	serpentine, carbonate, magnetite, clay	serpentine, carbonate, magnetite
Abundance of metamorphic veins	8.9%	1.2%	2.0%	1.9%	6.8%	3.1%	0.7%	1.8%

45 m. Hole 1271B was initiated 74 meters southwest of Hole 1271A on a similar, sedimented slope. Hole 1271B collapsed after drilling 104 m and the recovery of 16 m of core. Hole 1272A is located on the western flank of the Mid-Atlantic rift valley, near the summit of the inside corner high and just south of the 15°20′ Fracture Zone at a water depth of 2560 m. The inside corner high has been extensively dredged and surveyed by submersible dives [*Bougault et al.*, 1988, 1993; *Cannat*, 1993; *Cannat et al.*, 1992, 1997; *Cannat and Casey*, 1995; *Dosso et al.*, 1993; *Fujiwara et al.*, 2003], which have recovered numerous samples of dunite, harzburgite, and basalt. Hole 1272A was spudded into to a relatively flat area in the vicinity of several cliffs. The topmost 55 m of basement reveal numerous faults, intervals of poor recovery, and diverse lithologies, including fine-grained basalt, a medium-grained hypabyssal gabbro, and a carbonate cements breccia with serpentinite clasts. Most likely, the top portion of Hole 1272A represents a tectonic breccia with large blocks, up to 5 m in size. Below a fault gouge at 55 mbsf, 75 m of homogeneous, green, serpentinized harzburgite with minor dunite were drilled. Site 1274 is located on the western flank of the Mid-Atlantic rift valley at a water depth of 3940 m in an area of weathered outcrops along a gentle slope (Figure 1). Hole 1274A was penetrated to a depth of 156 mbsf, with a total core recovery of 35 m.

3. Results

3.1. Site 1268

[8] The 147.6 meter long section drilled at Site 1268 is composed of completely altered harzburgite and dunite that is intersected by mylonitic shear zones, late-stage magmatic dikes, and gabbronorite bodies that are moderately to completely altered (Figure 2a). The high recovery rate of Hole 1268A (53.3%) provides a unique opportunity to interpret the metamorphic evolution of the shallow mantle in the context of tectonic and magmatic events. The most important first-order observation is that two alteration events have affected the rocks: (1) pervasive serpentinization and (2) pervasive talc alteration, which overprints serpentinization in some sections. Both serpentinization and talc alteration were static and apparently unrelated to the intensity of crystal-plastic deformation [*Shipboard Scientific Party*, 2003].

[9] Peridotites are altered to green to dark green serpentinite consisting of serpentine+magnetite± pyrite that completely replace both olivine and orthopyroxene. Cr-spinel is fresh in most instances, although minor alteration to magnetite and rare ferritchromite is present locally. The microtextures of serpentinized harzburgite and dunite range from pseudomorphic mesh and hourglass textures to transitional ribbon textures to nonpseudomorphic interlocking textures with serrate chrysotile veins (Figure 3a).

[10] Talc alteration is remarkably common in the drill core from Hole 1268A. Talc-altered harzburgites reveal variable replacement of groundmass serpentine and bastite by talc (Figures 3b–3f). Incipient replacement of serpentine by talc is initiated along serpentine bands defining ribbon textures and mesh-rims (Figure 3b) or along microcracks in serpentinite (Figure 3c). Even in highly talc-altered rock the original serpentinite microtextures is commonly preserved (Figure 3d). In some completely talc-altered rocks recrystallization resulted in coarse-grained nonpseudomorphic talc patches. In talc-altered harzburgite with complete bastite replacement, dark green, mm-wide rims of relict serpentine of unusually intense green color and high birefringence outline the original shape of the orthopyroxene (Figure 3e). Textural evidence shows that talc alteration post-dates serpentinization, early chrysotile+magnetite veining, pyrite+serpentine veining, and later generations of chrysotile veins.

[11] The basement at Site 1268 is heavily veined (8.9 Vol.% veins in core), with a remarkably high abundance of sulfide and sulfide/oxide-bearing talc, serpentine veins, and monomineralic talc veins (Figure 3f). Sulfides and oxides are abundant (up to a few percent of individual cores) in the halos along these metamorphic veins as well as along gabbroic dikes. Different generations of serpentine veins are developed throughout Hole 1268A. A first generation of serpentine-magnetite veins was synchronous with the serpentinization of the harzburgites and dunites. Later generations of pyrite±serpentine veins followed by fibrous chrysotile veinlets within the serpentines are part of the early background serpentine alteration. Talc veins (Figure 3f) are the most common vein type in Hole 1268A, making up 48% of all veins by volume. Talc is also common as gangue in pyrite±polydymite±magnetite±hematite±millerite veins that post-date serpentine-magnetite veins

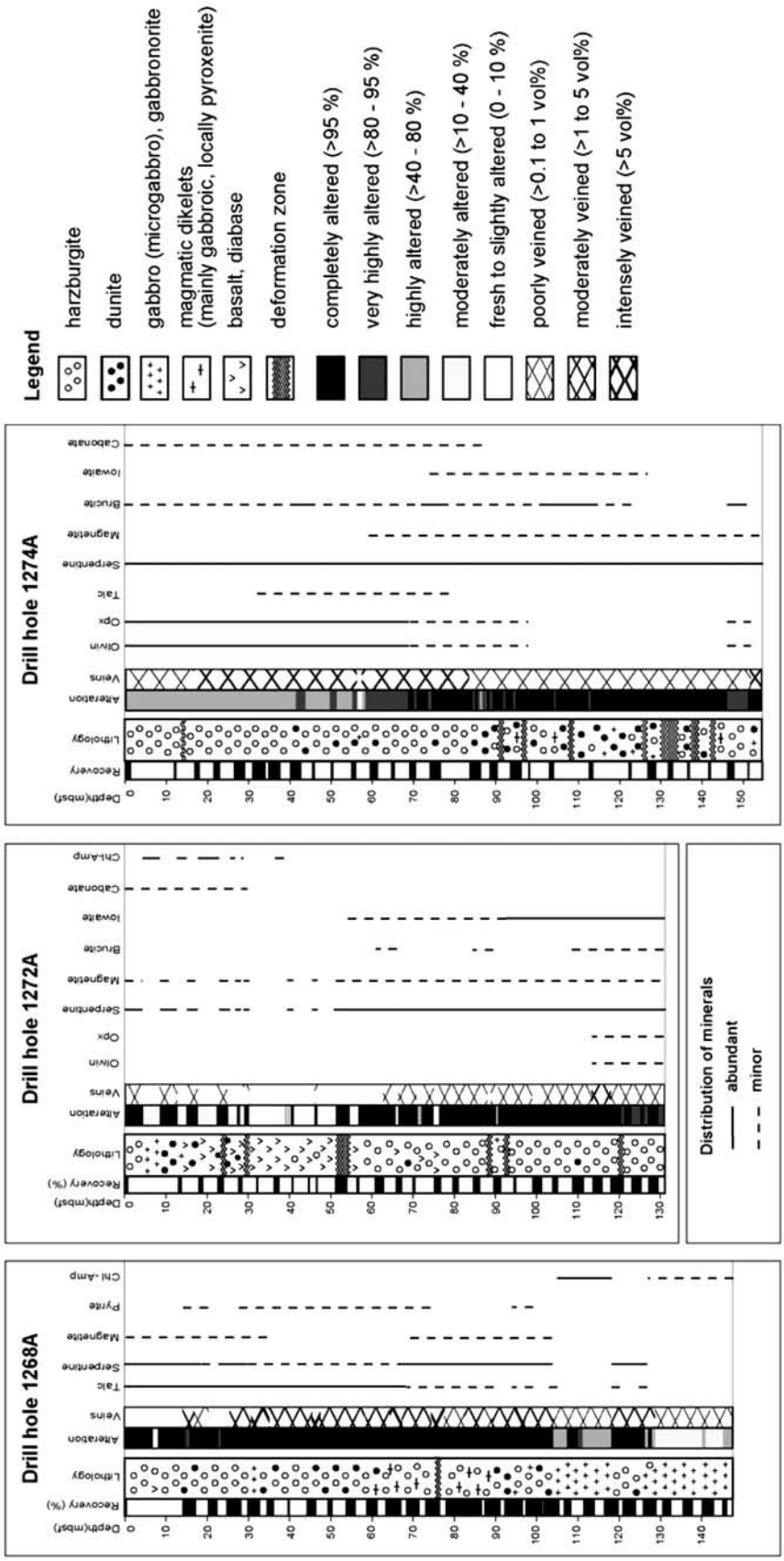

Figure 2. Lithologic columns for Holes 1268A, 1272A, and 1274A summarizing core recovery, principal primary lithology, intensity of alteration and veining, and secondary mineral distribution (from left to right in each panel). Opx, orthopyroxene; Chl-amph, chlorite and amphibole.

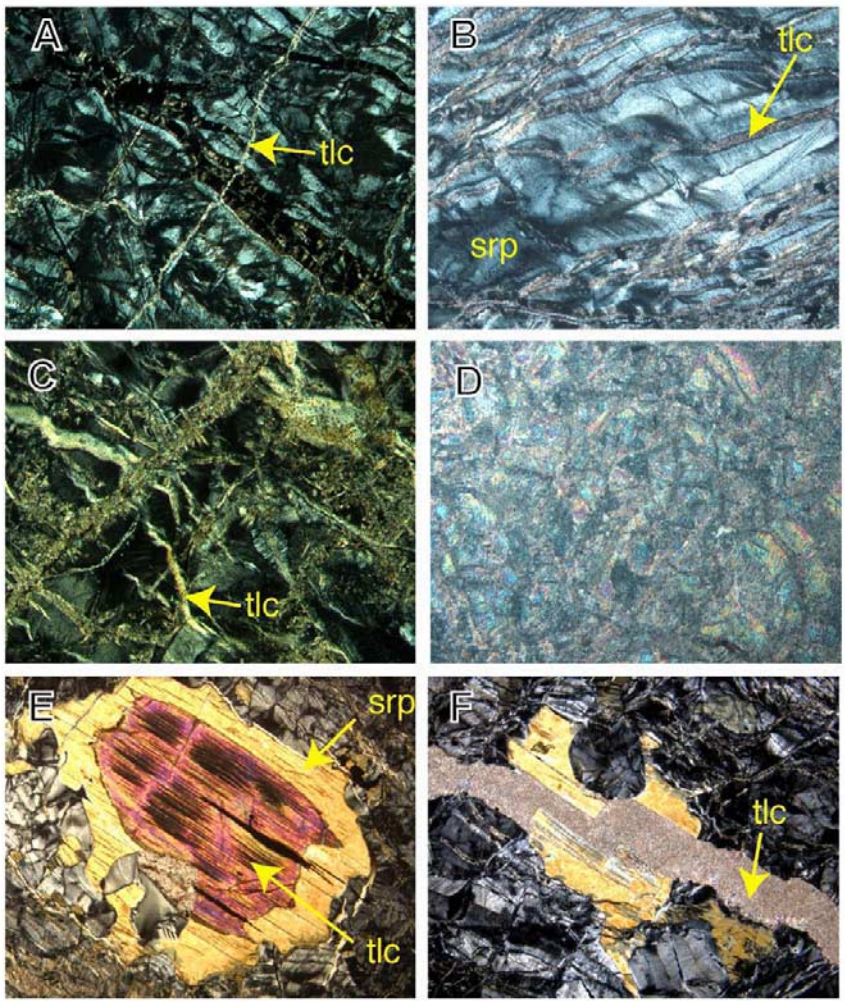

Figure 3. Photomicrographs of thin sections of rocks from Hole 1268A. (a) Nonpseudomorphic serpentinite texture in which mesh cells have coalesced to form ribbons. Crosscutting γ-serpentine veins (lower right to upper left) are cut by narrow, late talc veins (high birefringence). Sample 209-1268A-2R-2, 38–40 cm. (b) Ribbon-textured serpentinite with partial replacement of serpentine by talc following the orientation of the ribbons. Sample 209-1268A-4R-1, 124–127 cm. (c) Talc replacing serpentine along irregular vein networks that cut earlier chrysotile veins. Sample 209-1268A-12R-1, 47–49 cm. (d) Complete replacement of serpentine by talc, preserving the original (hourglass?) serpentinite microtexture. Sample 209-1268A-19R-1, 51–53 cm. (e) The core of an orthopyroxene crystal is replaced by pseudomorphic talc and pyrite (along cleavage) that is surrounded by a corona of unusually pleochroic serpentine. Both pseudomorphic talc and pleochroic serpentine are replaced by a late generation of nonpseudomorphic talc (center, bottom). Sample 209-1268A-13R-2, 3–6 cm. (f) Bastite (orthopyroxene transformed to pleochroic serpentine) cut by a talc vein and replaced along cleavage by talc. The talc vein also cuts chrysotile veins associated with background alteration. Sample 209-1268A-12R-3, 71–74 cm. Field of view of Figures 3a–3d is 1.4 mm, and that of Figures 3e and 3f is 2.7 mm. All images are crossed Nichols. Tlc, talc; srp, serpentine.

and are the most abundant sulfide-oxide vein type. Late-stage oxide-sulfide bearing veins in Hole 1268A are dominated by hematite indicating more oxidizing conditions. Late-stage carbonate veins are not present at all in the drill core from Hole 1268A. Although the timing of veining and alteration is complex in detail [*Shipboard Scientific Party*, 2003], the general sequence is early serpentine+magnetite±pyrite followed by late talc±pyrite±hematite.

3.2. Site 1270

[12] Harzburgites and dunites in Holes 1270A and 1270C were affected by pervasive serpentinization mostly under static conditions. Serpentinite micro-

textures are transitional with serrate chrysotile veins and ribbons of coalesced mesh and hourglass cells. Fine-grained magnetite is present, forming networks within the serpentinized matrix. Mesh-rim textures are preserved where serpentinization of olivine has not been complete and olivine is preserved in the centers of mesh cells.

[13] Where relict fresh olivine and orthopyroxene are preserved, orthopyroxene is partially replaced by talc±tremolite along the margins and along internal fractures. Talc±tremolite alteration locally overprints serpentinization but is largely restricted to zones of mafic dike intrusion and deformation. Partial weathering of relict olivine to clay and Fe-oxyhydroxides is common.

[14] In Holes 1270C and D there is an intimate association of serpentinized harzburgite and dunite with deformed, schlieren-shaped intrusions of completely altered gabbro. Within these deformed zones there is evidence for highly localized, syn-kinematic, high-temperature alteration. The vein assemblages in Holes 1270C and 1270D show complex relationships indicating that multiple episodes of veining took place after the deformation.

[15] Serpentinization is mostly static, but one sample from the uppermost part of Hole 1270A shows evidence for syn-kinematic serpentine recrystallization. There the serpentinite mesh texture is overprinted by shear zones that recrystallized to interpenetrating serpentine (Figure 4a). Furthermore, chrysotile veins are transposed into the foliation, indicating that deformation occurred during late-stage serpentinization. Pre- to syn-kinematic serpentinization in Holes 1270C and 1270D is reflected by the prominent development of paragranular serpentine veins (Figure 4b). Some en echelon cross-fiber serpentine veins are transposed and rotated in talc shear zones. However, late generations of serpentine veins crosscut talc-rich shear zones and earlier generations of serpentine veins, indicating that serpentinization took place in several stages and that deformation continued after the initial high-temperature ductile deformation. Hence, in different sections of cores from Site 1270, there is evidence for serpentinization prior to, during, and after the deformation recorded by amphibole-chlorite-talc schists.

[16] In addition to the main types of alteration described above, Holes 1270 C and 1270D contain minor carbonate and oxide veins. Networks of Fe-oxyhydroxide veins are generally restricted to the shallower sections of these holes and probably formed during seafloor weathering. The predominance of hematite and general lack of sulfides indicates oxidizing conditions and low sulfur fugacities. Carbonate veins with red clays also formed during shallow seawater infiltration. Carbonate crystals in these veins commonly display a prismatic habit, indicating aragonite that is formed by interaction with cold seawater [e.g., *Bonatti et al.*, 1980]. However, carbonate is locally present in the deeper part of Hole 1270D, where carbonate veins are spatially related to talc shear zones and cut serpentine textures. These veins do not cut across talc-rich shear zones, but appear to grade into them. Potentially, this relationship may indicate that the formation of carbonate is related to the circulation of carbonate-bearing fluids along the shear zones.

3.3. Site 1271

[17] Two holes were cored at Site 1271, which is located at the inside corner high of the Mid-Atlantic Ridge segment to the south of the 15°20′N fracture zone. The drill core from Hole 1271A consists predominantly of completely serpentinized dunite with localized occurrences of brucite. Some intervals also experienced low-temperature seafloor weathering. The drill core from Hole 1271B consists of a complex association of completely altered mafic rocks and variably altered dunite and harzburgite. The ultramafic rocks are intruded and infiltrated by the gabbroic lithologies that have experienced variable degrees of syn-deformational hydrothermal alteration to amphibolite. Relatively fresh dunite is also present, in particular in proximity to amphibolites.

[18] Hole 1271A is dominated by light gray to black, completely serpentinized dunites. Microtextures in the serpentinized dunite range from pseudomorphic mesh texture through transitional texture to nonpseudomorphic ribbon texture. In the uppermost 10 meters, the dunites have a yellowish-green to gray groundmass hosting abundant, transgranular, black serpentine-magnetite veins, mainly oriented parallel to the long axis of the core. This peculiar "tiger-striped" appearance is limited to the uppermost basement and is also common in dunite dredged from the seafloor (H. J. B. Dick, personal communication, 2003). The development of this macroscopic texture may hence relate to seafloor weathering reactions including brucite dissolution.

[19] Deeper in the section, completely serpentinized dunites have a uniform gray color and contain

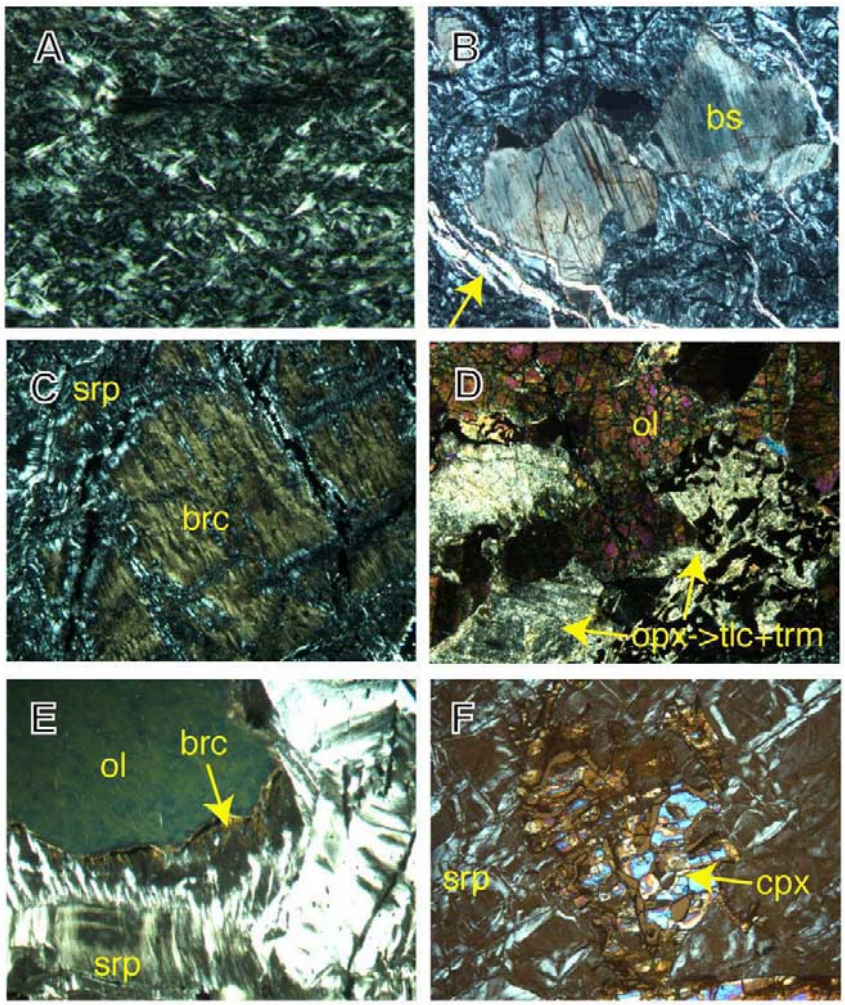

Figure 4. Thin section photomicrographs of rocks from Sites 1270, 1271, and 1274. (a) Interpenetrating serpentinite texture in a serpentine mylonite. Sample 209-1270A-1R-1, 35–38 cm. Field of view is 0.7 mm. (b) Bastite (bs) after orthopyroxene in protogranular serpentinized harzburgite with paragranular chrysotitle veins (arrow). Sample 209-1270C-1R-1, 36–39 cm. Field of view is 5.4 mm. (c) Brucite (brc) and serpentinite (srp) replacing olivine in a dunite. Sample 209-1271A-4R-2, 29–31 cm. Field of view is 1.4 mm. (d) Orthopyroxene is replaced by talc and tremolite (opx–>tlc+trm), while olivine (ol) is largely fresh. Sample 209-1271B-10R-1, 40–43 cm. Field of view is 2.7 mm. (e) Olivine (ol) is partly replaced by serpentine (srp) and brucite (brc). Sample 209-1274A-17R-1, 39–42 cm. Field of view is 0.7 mm. (f) Olivine in a dunite is completely serpentinized (srp), while clinopyroxene (cpx) intergrown with spinel is fresh. Sample 209-1274A-8R-1, 109–111 cm. Field of view is 1.4 mm. All images are crossed Nichols.

substantial proportions of brucite, locally up to 10–15 vol%. Brucite with anomalous brown interference colors forms aggregates of fine, elongate crystals that are surrounded by, and intergrown with serpentine (Figure 4c). This texture indicates that the brucite formed coeval with serpentine.

[20] Like in Hole 1271A, dunite comprises a greater proportion of the recovered core than harzburgite in Hole 1271B. Pervasively serpentinized dunite and harzburgite range in color from light to dark green in the uppermost two cores to gray and black in the deeper sections and are composed mainly of serpentine and magnetite. Brucite is locally abundant (up to 5%) as brown aggregates within the serpentine mesh texture. Noticeable amounts of brucite are consistently present near the bottom of the hole in Sections 1271B-17R-1 to 19R-1 (84–95 mbsf). Serpentinization textures vary from relict mesh texture, to ribbon textures, to shear zones in which a distinct

foliation is present. Locally, bastite pseudomorphs after orthopyroxene are present. Talc alteration is minor in Hole 1271B and is present only in three short intervals where it is clearly related to deformation (talc-tremolite schists). In relatively fresh dunites (chiefly in cores 12 and 13 of Hole 1271B), rare orthopyroxene is replaced by talc (Figure 4d), while olivine is mostly fresh. The predominance of dunite at Site 1271 differs from the relative proportions recovered at Sites 1268 and 1270, where harzburgite is more abundant than dunite.

[21] Amphibole-bearing dunites, in which the dunite is commonly relatively fresh, first appear at a depth of about 50 mbsf. The contacts between dunite and amphibole-bearing assemblages are variable and complex. The general impression is that of intrusions of mafic material into dunite, locally disaggregating it and engulfing cm-sized dunite fragments, while forming apophyses and veins in other sections of the core. Alteration of the dunite to serpentine begins along irregular cracks that form a mesh network, usually with fresh olivine in the mesh centers. Olivine is also replaced by amphibole, in particular in proximity to the contacts with mafic material. Amphibolitization of olivine is pseudomorphic and preserves the magnetite rims of mesh texture in olivine. Orthopyroxenes with vermicular spinel are altered to talc, even in relatively fresh dunite. It appears that dunite in contact with mafic material is much less serpentinized than dunite in sections of the core that do not contain mafic material.

3.4. Site 1272

[22] The lowermost 86 m of basement drilled at Site 1272 comprise serpentinized harzburgite and dunite, consisting of serpentine, and magnetite with variable amounts of brucite and/or iowaite (Figure 2b). The microtextures range from pseudomorphic mesh-rim textures to transitional ribbon textures to rare nonpseudomorphic interlocking textures. Microscopic, apparently fibrous, serpentine veins are common and include length-slow γ-serpentine (chrysotile) as well as length-fast α-serpentine veins (lizardite). The latter type of microveins was not observed in cores from any of the other Leg 209 drill sites. In the lowermost 31 mbsf of Hole 1272A, serpentinization of olivine and orthopyroxene was incomplete, and 1%–8% of these phases are preserved. The overall decrease in alteration intensity is matched by increases in density and sonic velocity in the bottom part of the hole [*Shipboard Scientific Party*, 2003]. In the uppermost 30 mbsf, oxidative alteration of serpentinized harzburgite and dunite to reddish brown clay, carbonate, and Fe-oxyhydroxide is abundant, in particular in proximity to carbonate-clay cemented fault breccias. A fault gouge deeper in the core (Figure 2b) lacks oxidative alteration.

[23] Two aspects of the alteration of ultramafic rocks in Hole 1272A are unusual. The first is that fine-grained magnetite-serpentine stringers, which are typically associated with replacement of olivine, are absent in samples from Hole 1272A. Instead, coarse magnetite is developed in the cores, rather than the mesh-rims, of the serpentine mesh texture. The second notable difference between serpentinites of Site 1272 and those from other sites is the abundance of soft, clayey serpentinized harzburgites and serpentine mud. Entire sections of the core were extremely soft and plastic when retrieved from the core barrel. After being exposed to air for more than a day, the core from these intervals developed shrinkage fractures and an overall crumbly appearance. In their most extreme form, these rocks have the appearance of mud. Characteristic peaks at 8.1 and 4.07 Å in x-ray diffractograms show that these samples contain iowaite. This communication is the first report of iowaite in serpentinites from a mid-ocean ridge setting. Iowaite is a rare hydrous magnesium hydroxide-ferric oxychloride, which was discovered in Precambrian serpentinite [*Kohls and Rodda*, 1967]. It has been recognized in ODP drill core of serpentinite mud volcanoes in the Izu-Bonin forearc [*Heling and Schwarz*, 1992] and from serpentinite at the Iberian margin [*Gibson et al.*, 1996]. The structure of iowaite is similar to brucite, however, it contains significant ferric iron and chlorine. On the basis of analyses by *Allman and Donnay* [1969] the structural formula is

$$\left[Mg(OH)_2\right]_4\ FeOCl \cdot nH_2O\ \ (n = 1 - 4).$$

All XRD analyses of samples from core 12 and further downhole show these peaks, with variable intensities, indicating that iowaite is present in the soft, visibly clay-altered serpentinites as well as in the hard serpentinite. In thin section, we noted brown patches of sheet-like aggregates with a poor polish that show wavy extinction of aggregates and straight extinction of individual pseudofibers.

3.5. Site 1274

[24] The dark gray to black harzburgites and dunites of Hole 1274A are highly to completely serpentinized and show a very homogeneous appearance throughout the hole. Alteration prod-

ucts include serpentine after olivine and orthopyroxene, brucite and magnetite after olivine, and minor talc and tremolite after clinopyroxene and orthopyroxene. Spinel is commonly fresh or slightly altered to magnetite. In partially serpentinized rocks, olivine is generally more altered than orthopyroxene. Clinopyroxene is commonly only moderately altered to talc and tremolite. In the uppermost 60 m of Hole 1274A, the degree of orthopyroxene alteration averages 50%–60%, while that of olivine is 80%. Olivine alteration in this interval produced only trace amounts of magnetite. Very highly to completely altered harzburgite and dunite from deeper in Hole 1274A show noticeable amounts of magnetite, commonly in diffuse magnetite-serpentine networks that appear to trace former olivine grain boundaries and cracks. Qualitatively, the downhole increase in the proportion of magnetite observed in thin sections appears to correlate with a downhole increase in magnetic susceptibility [*Shipboard Scientific Party*, 2003]. Brucite is usually present in dunite while in harzburgite it is either absent or present only in trace amounts.

[25] Nonpseudomorphic ribbon textures are very common in Hole 1274A and both mesh and ribbon textures are usually developed within single thin sections. Ribbon textures consisting dominantly of chrysotile (apparent fibers are length-slow) replace mesh textures, in particular in sections of the hole where paragranular chrysotile veins are abundant. Ribbon textures and paragranular chrysotile veins locally impose a foliated fabric on the rock.

[26] The ultramafic rocks from Hole 1274A show an interesting variety of microtextures. Specifically, three different types of mesh textures are developed: (1) mesh-rims of serpentine and magnetite, (2) relict kernels of olivine surrounded by serpentine and magnetite and brucite (Figure 4e), and (3) brucite kernels surrounded by serpentine and a trace of magnetite. Individual thin sections commonly show various combinations of these types of mesh texture. Unlike the fibrous brucite in Holes 1271A and 1271B, which could be clearly distinguished from fibrous serpentine on the basis of its optical orientation (length-fast), apparent fibers of brucite in thin sections of serpentinites from Hole 1274A are length-slow. Similar brown kernels were observed in mesh-textured serpentinites from the MARK area (Hole 920) and identified by electron microprobe analyses as finely intergrown brucite and serpentine [*Dilek et al.*, 1997]. The optical orientation of these aggregates suggests that the serpentine is lizardite. Direct replacement of olivine by lizardite and brucite (±magnetite) is common during serpentinization at relatively low temperatures around 200°C [e.g., *Sanford*, 1981; *O'Hanley*, 1996]. Thin sections in which olivine is completely serpentinized show fresh clinopyroxenes (Figure 4f). As we will discuss below, this relationship also indicates relatively low temperatures of fluid rock interaction (<250°C).

[27] Systematic downhole variations in the degree of serpentinization of ultramafic rocks were observed in Hole 1274A (Figure 2c). In the uppermost 100 m of the hole, the degree of alteration increases from 60%–70% to >95%. Between 60 and 95 mbsf, alteration intensities vary between 70% and 100%. Below a prominent fault gouge zone in Section 1274A-18R-2 at about 95 mbsf, alteration intensity is generally very high to complete (>95%). In the lowermost 2 m of core recovered from Hole 1274A, alteration intensities drop again slightly to values between 85% and 95%. These variations in the estimated degrees of alteration are mirrored by changes in bulk-rock density, thermal conductivity, compressional velocity and porosity [*Shipboard Scientific Party*, 2003].

[28] The uppermost 90 m of Hole 1274A are affected by oxidative seawater alteration forming prominent cm-wide reddish to brownish halos along carbonate veins, which account in some intervals for as much as 15 vol% of the hole. This type of alteration is commonly restricted to sections of core with white carbonate veins, although these are not always preserved and may have been broken off the margins of individual pieces during drilling.

4. Discussion

[29] Many oceanic serpentinites consist only of two phases: serpentine and magnetite. Determining the metamorphic evolution of these rocks is difficult, because fluid-mineral phase relationships cannot always be employed. The serpentinites from ODP Leg 209 are remarkable in this regard, as they are highly variable in their mineralogical composition and in the extents of serpentinization. Talc replaces serpentine at Site 1268, brucite is present in the variably serpentinized dunites from Sites 1271 and 1274, where orthopyroxene has reacted to talc, brucite and iowaite are developed in rocks from Site 1272, and a continuous transition from relatively fresh to completely serpentinized fresh harzburgites and dunite can be studied at Site 1274. The following discussion will evaluate the

observed phase relationships in the light of experimental [*Seyfried and Dibble*, 1980; *Janecky and Seyfried*, 1986; *Allen and Seyfried*, 2003] and theoretical [*Palandri and Reed*, 2004; *Wetzel and Shock*, 2000] constraints for seawater-peridotite interactions and under consideration of peridotite-hosted hydrothermal vent fluid compositions from the Logatchev, Rainbow, and Lost City hydrothermal sites [*Charlou et al.*, 2002; *Douville et al.*, 2002; *Kelley et al.*, 2001].

4.1. Serpentinite Phase Petrology

[30] Previous studies of oceanic serpentinites and associated gabbros from various settings [*Cannat et al.*, 1992; *Mével et al.*, 1991; *Hébert et al.*, 1990; *Bideau et al.*, 1991; *Früh-Green et al.*, 1996; *Dilek et al.*, 1997; *Prichard*, 1979; *Mével and Stadoumi*, 1996; *Agrinier et al.*, 1995; *Agrinier and Cannat*, 1997; *Schroeder et al.*, 2002] have revealed complex metamorphic evolution paths that include high-temperature (>300°–400°C) serpentinization and rodingitization and multiple lower-temperature overprints related to uplift and exposure of the mantle at the seafloor. In terms of their major components serpentinites are remarkably uniform, consisting of serpentine polytypes+magnetite± brucite±talc±tremolite [e.g., *Mével*, 2003].

[31] Temperature-pressure stabilities of serpentine phases are not well constrained. Thermodynamic calculations predict that antigorite is the stable serpentine phase above 200°–300°C and pressures below 2 kbar and that chrysotile and lizardite form from antigorite during low-temperature recrystallization [e.g., *Evans*, 1977]. An early oxygen isotope study of serpentinites is consistent with this view. *Wenner and Taylor* [1971] suggest that lizardite and chrysotile form at temperature below 235°C. However, more recent stable isotope investigations [*Agrinier et al.*, 1995; *Früh-Green et al.*, 1996; *Agrinier and Cannat*, 1997], field studies [*O'Hanley and Wicks*, 1995; *Wicks and Whittaker*, 1977], and hydrothermal experiments [*Normand et al.*, 2002; *Janecky and Seyfried*, 1986; *Allen and Seyfried*, 2003] indicate that lizardite and chrysotile form directly from olivine at temperatures above 300°C.

[32] The nature of the serpentine polytype is likely to be a function of temperature, fluid composition, P_{total}, $P(H_2O)$, and kinetics. While thermodynamical calculations predict that (at $P_{total} = P(H_2O) = 1$ kbar) antigorite forms at T > 300°C, lizardite forms at T < 200°C, and chrysotile forms at intermediate temperatures [e.g., *Evans*, 1977], stable isotope studies have shown that lizardite and chrysotile form at temperatures of 350–400°C [*Agrinier and Cannat*, 1997; *Agrinier et al.*, 1995; *Früh-Green et al.*, 1996]. Surface energy minimization effects may explain the metastable replacement of olivine by lizardite, followed by partial replacement of lizardite by chrysotile [*Normand et al.*, 2002]. *Sanford* [1981] and *O'Hanley* [1996] argue that the stability fields of lizardite and chrysotile may extend to higher temperatures if $P(H_2O) < P_{total}$. Actively serpentinizing systems within the oceanic lithosphere consume water, produce methane and hydrogen, and are likely at sub-lithostatic pressure, suggesting that $P(H_2O)$ is likely significantly smaller than P_{total}. The use of serpentine mineralogy in constraining the evolution of oceanic serpentinites is therefore somewhat problematic.

[33] The presence of incompletely serpentinized dunites and minor harzburgites at Sites 1271 and 1274 provides the opportunity to examine potential reaction paths of serpentinization. Field and experimental studies suggest that serpentinization at low to moderate temperature (<250°C) is a nonequilibrium process, during which dissolution of olivine proceeds at rates faster than precipitation of talc and serpentine [e.g., *Nesbitt and Brickner*, 1978; *Martin and Fyfe*, 1970].

[34] Figure 5a displays a Mg-Ca-Si-O-H mineral-fluid phase diagram for 200°C and 500 bars. The fluid composition will be driven toward the stability fields of serpentine and brucite, which represent the lowest energy mineral assemblage [e.g., *Hemley et al.*, 1977]. The reaction path proposed by *Nesbitt and Brickner* [1978] (black arrow in Figure 5a) is strongly curved, owing to rapid dissolution of olivine and consumption of acidity, followed by a shoaling of the trend due to dissociation of orthosilicate at high pH. The last part of the proposed reaction path is controlled by the forsterite dissolution boundary. If pH = 10 and silica concentrations of seawater are assumed (similar to the Lost City vent fluids [*Kelley et al.*, 2001]), the calculated silica activity at 200°C (the estimated maximum temperature of Lost City vent fluids [*Allen and Seyfried*, 2004]) is near the serpentine-brucite boundary in Figure 5a. However, the in situ pH at 200°C for the Lost City fluids (room temperature pH values around 10.5 [*Kelley et al.*, 2001]) is only 7.7. Still the Lost City fluid could be multiply saturated in olivine, brucite, and serpentine phases if the Mg^{+2} activity is $\leq$1 μmol/kg. Also shown in Figure 5a is a schematic reaction path for fluids

from a harzburgite-seawater interaction experiment [*Seyfried and Dibble*, 1980] that trends toward the chrysotile-brucite boundary. In contrast, fluids from a lherzolite-seawater experiment at 200°C and 500 bars [*Janecky and Seyfried*, 1986] do not evolve toward brucite saturation, because the high abundance of pyroxenes keeps the fluid pH low and the silica activity of the fluids high (Figure 5a). The fluid reaction path is therefore a function of both the reaction temperature (i.e., the relative rates of olivine and pyroxene alteration) and the modal composition of the peridotite.

[35] The effect of pyroxene on solution chemistry is even stronger at higher temperatures (>250°–300°C), where pyroxenes react faster than olivine [*Martin and Fyfe*, 1970; *Allen and Seyfried*, 2003]. Figure 5b demonstrates that high-temperature (365°C) black smoker fluids from the Logatchev and Rainbow peridotite-hosted hydrothermal systems [e.g., *Charlou et al.*, 2002], when respeciated at 400°C and 500 bars, are pinned by fluid saturation in pyroxene and that talc and possibly tremolite should form at the expense of pyroxene. As long as pyroxenes are present (and dissolve fast) the pH of the interacting fluids is low and the silica activity high [cf. *Allen and Seyfried*, 2003]. Only when the fluid is no longer pyroxene saturated can it evolve to higher pH and lower silica activity.

[36] These mineral-fluid phase relationships are relevant for the interpretation of the serpentine-brucite and olivine-amphibole-talc assemblages observed in cores from Sites 1271 and 1274. A possible interpretation of the relatively fresh dun-

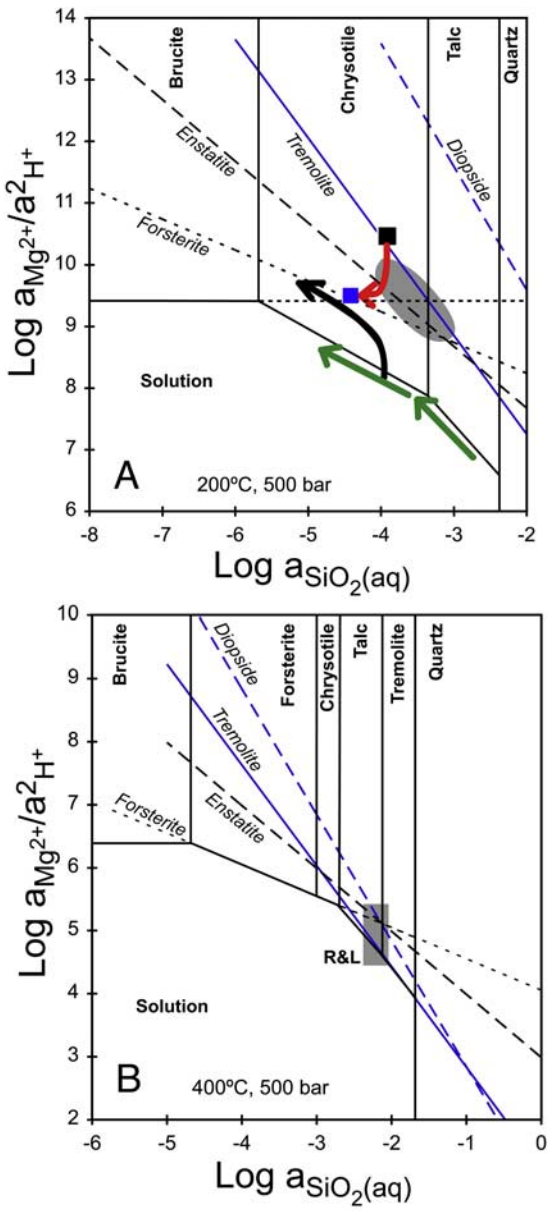

Figure 5. (a) Mineral-fluid phase diagram for the system Mg-Ca-Si-O-H at 200°C and 500 bars (right), constructed using thermodynamic data from *Johnson et al.* [1992] and assuming Log(aCa^{2+}/a^2H^+) = 6. The black trend is a hypothetical evolution path of fluids dissolving olivine at a higher rate than hydrous mineral are precipitated. The drop in silica activity is solely the result of the decrease in the orthosilicate activity coefficient as a function of increasing pH (calculated with SUPCRT92 [*Johnson et al.*, 1992]). The blue square represents the hydrothermal fluids from the Lost City vent site [*Kelley et al.*, 2001], respeciated for 200°C [*Allen and Seyfried*, 2004]. The in situ pH value of Lost City fluids at 200°C is 7.7; silica concentration is similar to seawater [*Kelley et al.*, 2001]. The Lost City fluids could be multiply saturated in olivine, brucite, and serpentine, if the Mg^{+2} activity is $\leq$1 μmol/kg. The gray field encompasses fluid compositions from a lherzolite-seawater reaction experiment at 200°C and 500 bars conducted by *Janecky and Seyfried* [1986]. Fluids from a harzburgite-seawater interaction experiment [*Seyfried and Dibble*, 1980] evolve along a trend indicated by the green arrows toward the chrysotile-brucite boundary. The black arrow is a hypothetical evolution path of a solution that dissolves olivine faster than it precipitates serpentine [cf. *Nesbitt and Brickner*, 1978]. The red arrow represents a schematic fluid evolution path for seawater heated to 200°C followed by a drop in Mg and an increase in pH. (b) Mineral-fluid phase diagram for the system Mg-Ca-Si-O-H at 400°C and 500 bars. The gray field labeled "R&L" represents fluid compositions from the Rainbow and Logatchev hydrothermal sites, respeciated for 400°C and 500 bars [*Charlou et al.*, 2002]. In situ pH values at these systems range between 4.5 and 5. Silica activities are 6 to 7 mmol/kg, and Mg^{2+} activity is assumed to be on the order of 0.1 mmol/kg.

ites with rare, talc-altered orthopyroxene pseudomorphs is that these rocks reacted with hydrothermal fluids at high temperatures (>300°C), where orthopyroxene reacts faster than olivine. The proximity of mafic material (amphibolites) to intervals of unaltered dunite may suggest that the presence of pyroxene and amphibole kept the silica activity of the interacting fluids high so that serpentinization of olivine was inhibited. Formation of talc after olivine is thermodynamically favored (Figure 5b) but kinetically sluggish [e.g., *Nesbitt and Brickner*, 1978]. Replacement of orthopyroxene by talc, on the other hand, is commonly observed in alpine and abyssal serpentinites [e.g., *Aumento and Loubat*, 1971; *Hostetler et al.*, 1966]. As the system moves toward lower silica activities after pyroxenes are exhausted, talc that had formed during initial alteration will react to serpentine. These processes explain the scarcity (or complete lack) of talc as part of the background alteration in many completely serpentinized rocks.

[37] The brucite-bearing dunites (and minor harzburgites) require a different genetic model (see Figure 5a). The phase relations indicate that these lithologies reacted with fluids of high pH and low silica activities. Such fluids are generated when alteration is controlled by rapid olivine dissolution and relatively sluggish hydrous mineral precipitation. Thermodynamically and kinetically, conditions for brucite-serpentine formation are favorable at low temperatures and in the absence of pyroxenes. The abundance of brucite at Site 1271 may suggest that the circulating fluids are dominantly high pH and low silica activity, which could be explained if the basement consists dominantly of dunite.

[38] At Site 1274, magnetite is rare where serpentinization is incomplete (as low as 60%), suggesting that significant magnetite formation does not begin until more than 60% of the primary rock is serpentinized. At Site 1274 brucite is most common in dunites, but does also occur in harburgites. Brucite is not expected to be associated with the breakdown of pyroxene, because the high silica activity of fluids reacting with pyroxene would prevent brucite formation and would cause previously formed brucite to react to serpentine according to reaction:

$$3Mg(OH)_2 + 2SiO_2(aq) = Mg_3Si_2O_5(OH)_4 + H_2O.$$

[39] The occurrence of both brucite and partially serpentinized pyroxene may hence indicate local disequilibria during the main stage of serpentinization. Alternatively, the formation of serpentine+brucite+magnetite after olivine took place at a later stage, at temperatures below 250°C. The following reaction can possibly account for this observation:

$$3Mg_{1.8}Fe_{0.2}SiO_4 + 4.1\ H_2O = 1.5\ Mg_3Si_2O_5(OH)_4 + 0.9Mg(OH)_2 + 0.2\ Fe_3O_4 + 0.2H_2(aq).$$

[40] The molar volumes of brucite, magnetite, and chrysotile are 26.43 cm^3, 44.52 cm^3, and 108.5 cm^3, respectively [*Helgeson et al.*, 1978], so that the stoichiometry of this reaction corresponds to a mode of 83% serpentine, 12% brucite, and 5% magnetite (83:12:5).

[41] While here magnetite accompanies serpentine and brucite and appears to form directly from olivine breakdown, little magnetite is produced during initial serpentinization. Allowing for Fe to substitute for Mg in serpentine and brucite, e.g.,

$$3Mg_{1.8}Fe_{0.2}SiO_4 + 77/18\ H_2O = 1.5\ Mg_{2.9}Fe_{0.1}Si_2O_5(OH)_4 + 7/6\ Mg_{0.9}Fe_{0.1}(OH)_2 + 1/9Fe_3O_4 + 1/9H_2(aq)$$

will increase the proportion of brucite and decrease the proportion of magnetite (83:15:2). The formation of magnetite and H_2,aq maybe omitted altogether if Fe-rich brucite and serpentine are formed:

$$3Mg_{1.8}Fe_{0.2}SiO_4 + 4.5\ H_2O = 1.5\ Mg_{2.8}Fe_{0.2}Si_2O_5(OH)_4 + 1.5\ Mg_{0.8}Fe_{0.2}(OH)_2.$$

Hence the amount of magnetite, brucite, and H_2,aq formed depends upon the degree of Fe-incorporation into secondary phases.

[42] To explain density-magnetic susceptibility relationships in variably serpentinized harzburgites from ophiolites, *Toft et al.* [1990] suggested that initial serpentinization produces Fe-rich serpentine and Fe-rich brucite, and that magnetite forms during recrystallization of these phases as serpentinization proceeds. We tentatively propose a similar explanation for the observation that little magnetite is formed during initial serpentinization at Site 1274. However, we note that analyses of recrystallized serpentine from MARK serpentinites [*Dilek et al.*, 1997] have much higher Fe contents (5.2 ± 1.0 wt.% FeO) than pseudomorphic serpentine (2.8 ± 1.2 wt.% FeO). Our observation of direct replacement of olivine by serpentine, brucite AND magnetite that, as argued above, likely occurred subsequent to the initial serpentinization and possibly represents lower reaction temperatures pro-

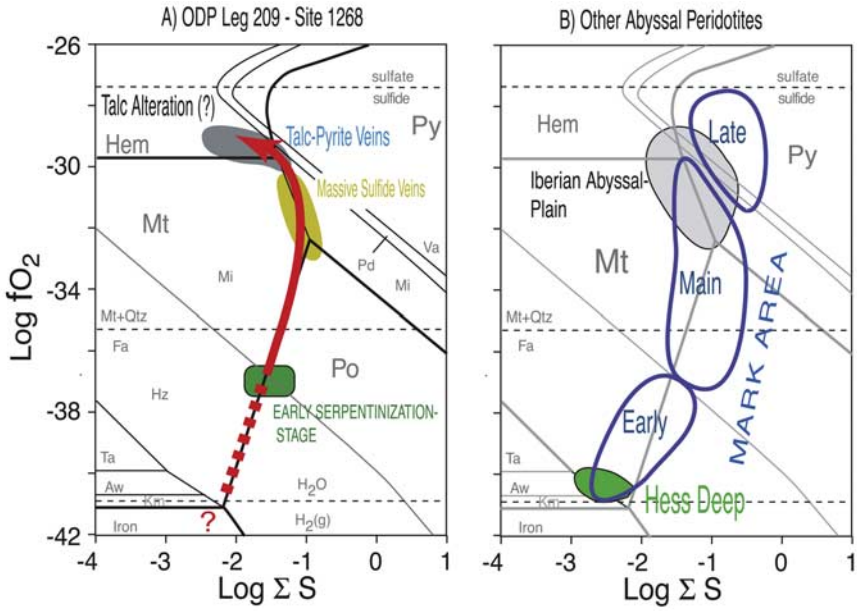

Figure 6. Phase diagram for the Fe-Ni-S-O system at 300°C and 2 kbar. Phase boundaries of Fe phases are marked by thick lines, those of Ni phases and Ni-Fe alloys are thin lines, and others are dashed lines. Fe phases are hematite (Hem, Fe_2O_3), pyrite (Py, FeS_2), magnetite (Mt, Fe_3O_4), pyrrhotite (Po, $Fe_{1-x}S$), and Ni- and Ni-Fe phases are vaesite (Va, NiS_2), polydymite (Pd, Ni_3S_4), millerite (Mi, NiS), heazlewoodite (Hz, Ni_3S_2), taenite (Ta, δFeNi), awaruite (Aw, Ni_3Fe), and kamacite (Ka, αFeNi). Oxide-sulfide phase boundaries simplified after *Frost* [1985]; others are calculated with SUPCRT92 [*Johnson et al.*, 1992]. (a) Fields mark oxide-sulfide assemblages observed in Hole 1268A, and the red arrow is the inferred evolution path. (b) Fields mark oxide-sulfide assemblages observed in Hess Deep and MARK areas [*Alt and Shanks*, 1998, 2003].

vides an alternative explanation for the increased magnetite formation during advanced stages of serpentinization. The presence of fresh clinopyroxene in rocks in which olivine is completely serpentinized (Figure 4f) can also best be explained by main stage alteration at temperatures at which olivine reacts much faster than pyroxene (<250°C).

4.2. Redox Conditions

[43] While the sequence of alteration reaction observed in Hole 1274A and previous studies [e.g., *Toft et al.*, 1990] suggest that magnetite formation peaks when most of the rock is serpentinized, ongoing fluid-rock reactions after serpentinization is complete may lead to magnetite destruction. This is clearly demonstrated by the rocks recovered from Site 1268 that show reaction of serpentine and magnetite to talc and hematite along with a decrease in magnetic susceptibility [*Shipboard Scientific Party*, 2003]. The succession of oxide/sulfide minerals in Hole 1268A indicates the development of the rock-fluid system to more oxidizing conditions with time (Figure 6a). The presence of magnetite in veins as well as the occurrence of reduced Fe and Ni sulfides (relict pyrrhotite/pentlandite and partial replacement by heazlewoodite) in a moderately altered orthopyroxenite suggest fairly reducing conditions during early serpentinization and veining. Phases indicating even lower oxygen fugacities, found in peridotites from Hess Deep and MARK area [*Alt and Shanks*, 1998, 2003] (Figure 6b), were not identified in the course of our limited shipboard studies. Increasing modal percentages of hematite in the late stage veins are associated with decreasing H_2S(aq) and H_2(aq) activities of the interacting hydrothermal solution (Figure 7). Such a trend can be expected in long-lived hydrothermal systems where the reducing capacity of the rock is exhausted by oxidation of seawater sulfate [e.g., *Seyfried and Ding*, 1995]. This scenario is consistent with the observation that the peridotites in Hole 1268A underwent multiple episodes of intense and pervasive alteration under variable redox and pH conditions. This is generally similar to serpentinites from the Iberian Abyssal Plain [*Beard and Hopkinson*, 2000; *Hopkinson et al.*, 2004].

[44] The late-stage veins are dominated by hematite and not by pyrite like in other locations [*Alt and Shanks*, 1998, 2003] (Figure 6b). *Seyfried and*

Ding [1995] suggest that the reaction anhydrite + 3 anorthite + 4 H_2(aq) = 2 clinozoisite + H_2S(aq) + $2H_2O$ (AAC) keeps the system fairly reducing until plagioclase has been reacted to albite (and anorthite activity is small). This model can explain the lack of hematite in reaction zones of basalt-hosted hydrothermal systems [e.g., *Alt*, 1995]. In peridotite-hosted systems a Ca-Al silicate/anhydrite buffer may not be affective. In any case, high Ca concentrations (20–65 mM [*Charlou et al.*, 2002; *Kelley et al.*, 2001]) in fluids venting from peridotites indicate that enough Ca is released from the incompletely serpentinized rocks to keep sulfate level low. One way of simulating the effect of intense water rock reaction on redox equilibria is assuming a drop in anorthite activity along with decreasing temperatures of fluid-rock interaction as the crust is uplifted. The consequence of a coupled drop in temperature and anorthite activity (Figures 7a–7c) is a shift of the AAC equilibrium relative to hematite-magnetite-pyrite such that below 300°C hematite may coexist with anhydrite. Another way of explaining the shift in redox equilibria is independent of a possible CaAl-silicate/anhydrite buffer. Seawater has insufficient Ca contents (10 mM) to precipitate all the sulfate (28 mM) as anhydrite upon heating. In basalt-hosted hydrothermal systems sulfate is near-zero, because Ca is rapidly released to the fluid in the downwelling limb of a convection cell and sulfate is controlled by anhydrite solubility. However, Ca release from peridotite may be diminished if the protolith is strongly melt-depleted and/or the rock is completely serpentinized and Ca-leached. If such a rock undergoes continued reaction with seawater, sulfate may remain in the fluid at higher concentration levels and hematite may become stable. The temperature-dependent shift of the sulfate/sulfide equilibria relative to that of the hematite/magnetite boundary (Figure 7) indicates that acidic fluids with significant sulfate contents may coexist with hematite at temperature of 300°C and below. Slightly alkaline fluids (e.g., in situ pH of 7.5–8), such as at the Lost City site, cannot equilibrate with hematite (dashed, gray line in Figure 7) even if sulfate is present. This is consistent with our earlier suggestion that olivine reacts to serpentine, brucite, and magnetite at high fluid pH that is expected to evolve when olivine reacts faster than pyroxene. At

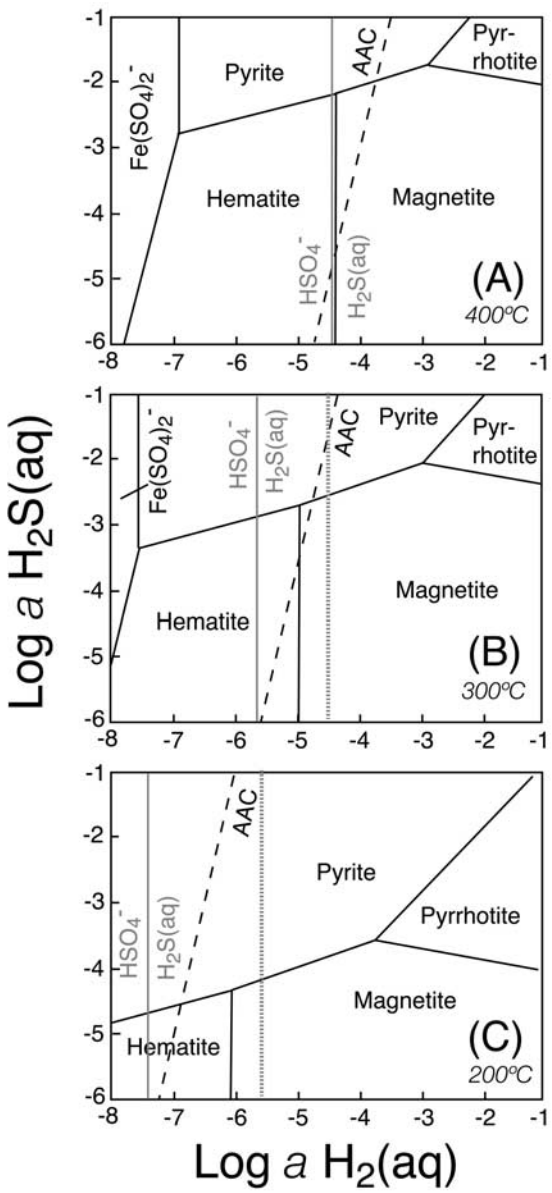

Figure 7. Mineral fluid phase diagram for the system Fe-H-O-S at temperatures of (a) 400°C, (b) 300°C, and (c) 200°C and a pressure of 1 kbar. The dashed line labeled AAC is for the reaction anhydrite + 3 anorthite + 4 H_2(aq) = 2 clinozoisite + H_2S(aq) + $2H_2O$. Anorthite activity is (a) 0.7, (b) 0.5, and (c) 0.3. Note that the presence of anhydrite excludes hematite at temperatures >300°C, while anhydrite and hematite may coexist at lower temperatures. Gray lines are for equal activities of HSO_4^- and H_2S(aq) (continuous) and for equal activities of HS^- and SO_4^{2-} (dashed). The latter sulfide-sulfate species are more relevant at higher pH. The continuous gray lines are for calculated in situ pH values for Rainbow fluids (200°C: 3.0; 300°C: 3.9; 400°C: 4.6) and Lost City (200°C: 7.7; 300°C: 7.5) based on 25°C pH values of 2.8 (Rainbow [*Charlou et al.*, 2002]) and 10.5 (Lost City [*Kelley et al.*, 2001]). Note that the sulfate-sulfide boundary shifts to the left more rapidly than the hematite-magnetite boundary as temperatures decrease. Also note that in the presented temperature range sulfate and hematite may not coexist at high pH values relevant for Lost City. All calculations are based on the SUPCRT92 database [*Johnson et al.*, 1992].

Site 1268, olivine is completely reacted out. Therefore circulating seawater will not become alkaline and may produce hematite upon interaction with serpentinite. These examples illustrate the complex relations between water-silicate reactions, fluid chemistry, and redox equilibria in peridotite-hosted hydrothermal systems.

4.3. Si Metasomatism of Serpentinites at Site 1268

[45] The most unusual aspect of the hydrothermal alteration at Site 1268 is the widespread replacement of serpentine by talc under static conditions. Replacement of serpentinized peridotite and gabbro by talc has been reported before. *Escartín et al.* [2003] documented the widespread presence of amphibole-chlorite-talc schists on rift valley walls in the 15°20′N area that represent a late stage of high-temperature syntectonic alteration along detachment faults. *Früh-Green et al.* [2003] mention talc-rich lithologies from the detachment fault surfaces at Atlantic Massif at the MAR 30°N. *D'Orazio et al.* [2004] describe talc-rich serpentinite and gabbro breccias and talc schists from the St. Paul and Conrad fracture zones in the Atlantic. All these occurrences have been attributed to large volume fluid flux along faults leading to Si metasomatism. The unusual aspect about the talcous rocks from Site 1268 is complete replacement of serpentine by talc under static conditions.

[46] Another remarkable observation is the lack of Ca metasomatism (rodingitization) of the gabbros and gabbroic veins encountered in Hole 1268A. In previously drilled and dredged sections of upper mantle [*Dilek et al.*, 1997; *Früh-Green et al.*, 1996; *Bideau et al.*, 1991] gabbros are Ca-metasomatized, and it has been suggested that Ca released during serpentinization is fixed in Ca silicates replacing primary minerals of the gabbro. This static Ca metasomatism of gabbros embedded in peridotite is common elsewhere, but it is not developed at Site 1268, where, instead, serpentinites have undergone pronounced Si metasomatism.

[47] It is well documented that talc forms after orthopyroxene under static conditions during prograde serpentinization and is replaced by lizardite either during retrograde serpentinization [*Wicks*, 1984] or due to a combination of increased H_2O activity and decreased silica activity in the fluid [*Frost*, 1985]. As discussed in the previous section the formation of noticeable amounts of early talc and tremolite (after orthopyroxene) and brucite (after olivine) during prograde serpentinization is consistent with field observations, experimental results and vent fluid chemistry. Hydrothermal experiments (at 400°C and 500 bars) confirm that fluids are talc-saturated as long as fresh pyroxene is left in the serpentinizing peridotite [*Allen and Seyfried*, 2003]. Similarly, brucite is believed to be a product of incipient serpentinization which, due to reaction with aqueous SiO_2 released by the breakdown of orthopyroxene to lizardite, forms lizardite and magnetite [e.g., *Toft et al.*, 1990].

[48] There is no relict talc, tremolite, or brucite in serpentinites from Hole 1268A, suggesting that serpentinization reached an advanced stage, at which only serpentine and magnetite were present. Another indication of the advanced degree of serpentinization in Hole 1268A is the general scarcity of pseudomorphic mesh textures and the common development of transitional hourglass and ribbon textures [*O'Hanley*, 1996]. Furthermore, interlocking textures, indicating recrystallization of mesh-textured serpentine, are common and serrate chrysotile veins formed at the expense of early lizardite.

[49] The replacement of serpentine by talc at Site 1268 is a metasomatic process. Fresh Harzburgite (80%olivine, 20% orthopyroxene) has a molar (Mg+Fe)/Si of 1.8. Serpentine has a molar (Mg+Fe)/Si of 1.5 so that some transfer of Mg, Fe, and Si must be inferred unless the rock contains abundant brucite [*O'Hanley*, 1996]. The molar (Mg+Fe)/Si of talc is 0.75, and hence the complete replacement of serpentine by talc in long sections of core from Hole 1268A indicates substantial mass transfer of Mg, Fe, and Si. Mg solubility in hydrothermal fluids is extremely low in the presence of hydrous Mg-silicates [e.g., *Saccocia et al.*, 1994]. We calculate that at 150°–350°C and 1 kbar, the Mg concentration of 3.2 wt.% NaCl solution saturated with talc is less than 5 ppm at pH $\geq$ 6. To explain the replacement of serpentine ($\sim$40 wt.% Mg) by talc ($\sim$29 wt.% Mg) with Mg loss would require unreasonable high water-to-rock ratios >20,000. However, the solubility of Mg is strongly pH-dependent, and Mg solubility in talc-saturated seawater at 200°C is $\sim$100 ppm at pH = 5 and $\sim$10,000 ppm at pH = 4 (at an assumed silica activity of 1 mM). It is conceivable that seawater recharging into highly Ca-depleted peridotite cannot leach sufficient Ca^{+2} from the rock to balance the loss in Mg^{+2}, which is then in part balanced by the release of protons to the fluid. If the pH was indeed $\leq$5, Mg loss may attribute to the replacement of serpentine by talc. Marcasite is expected to

form at pH $\leq$ 4–5 [*Murowchick and Barnes*, 1986], and ongoing studies of Hole 1268A sulfide petrology will focus on the identification of marcasite in talc-altered rocks.

[50] One plausible reaction between serpentine and fluid to form talc is

$$Mg_3Si_2O_5(OH)_4 + 2SiO_2(aq) = Mg_3Si_4O_{10}(OH)_2 + H_2O,$$

which proceeds to the right if the silica activity of the fluid is increased and/or if the water activity is lowered. In some cases, the formation of talc-magnesite rocks after serpentinite have been a consequence of lowering the water activity of the fluid by adding CO_2 [e.g., *Peabody and Einaudi*, 1992]. However, we did not observe magnesite (or other carbonates) in detectable amounts and conclude that carbonatization cannot account for the abundant development of talc after serpentine. It is hence more likely that an increase in silica activity is responsible for the conversion of serpentine to talc. Talc alteration may therefore more likely be a result of Si metasomatism.

[51] The close spatial association of talc alteration and gabbro intrusions suggests that gabbro emplacement and talc alteration are related. Gabbro intrusion and dike formation in serpentinite could revive hydrothermal circulation by providing a heat source and creating permeability. However, hydrothermal circulation long after gabbro emplacement could also transport SiO_2 from gabbro into host peridotite. Theoretical geochemical models suggest that, at 350°C and 500 bars, mafic rock-seawater reactions form hydrothermal fluids that many orders of magnitude higher in silica and lower in pH than hydrothermal fluids produced by reaction of seawater with ultramafic rocks [*Wetzel and Shock*, 2000]. Hydrothermal reaction between gabbro and seawater under greenschist-facies conditions transform pyroxene and plagioclase in the gabbros to chlorite, amphibole, and talc, releasing silica and acidity and causing Si metasomatism and talc formation in the serpentinites. Serpentinization of olivine at 350°C and 500 bars is associated with extremely low silica concentrations (<0.01 mM) in the interacting fluids [*Wetzel and Shock*, 2000]. However, *Allen and Seyfried* [2003] have demonstrated that ultramafic rock alteration under conditions under which pyroxenes react faster than olivine may generate fluids with moderate Si concentrations (4 mM). Breakdown of pyroxene during harzburgite-seawater reactions is therefore an alternative (or additional) source of silica. Similarly, the abundance of hydrothermal sulfides in Hole 1268A may suggest input of hydrothermal sulfide derived from a gabbro-driven hydrothermal system as proposed by *Alt and Shanks* [2003] for serpentinites from the MARK area.

[52] While serpentinites at Site 1268 show extreme Si metasomatism, the gabbroic dikes lack rodingitization. Rodingitization commonly takes place when gabbros and ultramafic rocks undergo the same metamorphic history and Ca-rich fluids generated during serpentinization metasomatize the gabbros replacing pyroxene and plagioclase by diopside, tremolite, clinozoisite, prehnite, and hydrogrossular [e.g., *Schandl et al.*, 1989; *O'Hanley*, 1996]. The lack of rodingitization (even in small gabbroic veins) may also relate to the Ca-poor nature of the host peridotite.

4.4. Late-Stage Fluid-Rock Interactions

[53] The latest stages of veining in the Hess Deep, MARK, and Lost City areas is the formation of aragonite veins under ambient conditions at or near the seafloor [e.g., *Früh-Green et al.*, 2003; *Blusztajn and Hart*, 1996; *Dilek et al.*, 1997]. There is also abundant late-stage aragonite in serpentinites from the Iberian margin drill cores [*Hopkinson et al.*, 2000]. A variety of late-stage, low-temperature reactions is recorded in ODP Leg 209 drill core. The late-stage talc overprint and sulfide/oxide veining at Site 1268 likely took place at somewhat elevated temperatures. Aragonite veins were not identified in core from Hole 1268A, suggesting that present-day veining and seawater ingress may be minimal, or that exposure at the seafloor was recent. At other sites (in particular 1271 and 1274), aragonite veining and low-temperature oxidative alteration of relict primary phases is common.

[54] The discovery of iowaite in core from Hole 1272A is the first reported occurrence of this phase from a mid-ocean ridge setting. It has been inferred that iowaite may be formed from iron-bearing brucite under oxidizing conditions [*Heling and Schwarz*, 1992]. This process involves the oxidation of Fe^{2+} in brucite to Fe^{3+} generating a charge imbalance, which is accommodated by incorporation of Cl^- between brucite layers. In a model suggested for iowaite formation in serpentinite muds in the Izu-Bonin forearc this reaction is proposed to take place immediately below the seafloor due to infiltration of ambient seawater [*Heling and Schwarz*, 1992]. Conversely, occurrences of iowaite in serpentinites from the Iberian margin (ODP Site 897) have been related to circulating low-temperature, seawater derived

Cl-rich brines [*Gibson et al.*, 1996]. Here, iowaite is restricted to a zone with elevated Cl-concentrations in bulk rock analyses (up to 1 wt%) and it is inferred that alteration is this area was probably independent of the earlier serpentinization, sulfidization and pyrite formation, and later surficial oxidative alteration.

[55] The observation of abundant iowaite distinguishes Hole 1272A from all other holes drilled during Leg 209. A distinctive stage of alteration, postdating serpentinization, may have occurred in this area which may have been associated with fluid flow along the major fault zones observed in this hole. While the involvement of a brine in the formation of iowaite is questionable, iowaite does indicate oxidizing conditions. It is remarkable to find long sections of basement that have been oxidized given the fact that fluids actively venting from oceanic core complexes and ultramafic massifs in ophiolites are enriched in aqueous H_2 [*Kelley et al.*, 2001; *Neal and Stanger*, 1983; *Abrajano et al.*, 1988]. It has been proposed that H_2 is generated under a range of temperatures by hydrolysis on ferrous oxide in olivine [*Neal and Stanger*, 1983; *Holm and Charlou*, 2001]. The hydrogen will react (possibly catalyzed by microbial activity) with dissolved oxygen, nitrate, and sulfate. As long as fresh olivine is present, the interacting fluids should hence be anoxic. There are small amounts of fresh olivine present in the interval of iowaite occurrence in Hole 1272A. Maybe the basement Site 1272 is effectively hydrated so that circulating fluids do not react with sufficient amount of fresh material to produce significant H_2,aq.

[56] The presence of nontronite in serpentine muds recovered from Hole 1274A also indicates that water-rock reactions continued at low temperatures and under oxidizing conditions. This is also suggested by the development of aragonite veins with oxidation halos in the uppermost 90 m of Hole 1274A. The aragonite veins disappear abruptly below the first fault gouge at 95 mbsf. Either the fault gouge represents a hydrogeological barrier that prevents cold seawater from penetrating deeper into the basement, or the fault zone accommodates the strain so that fracturing and circulation of cold seawater is limited to the hanging wall of the gouge.

5. Conclusions

[57] ODP Leg 209 drill core reveals peridotite-seawater interactions that took place under a wide range of temperature, pH, and redox conditions and involved fluids with variable silica activities. It is apparent that apart from the physicochemical conditions of peridotite-seawater reactions, protolith composition, presence of gabbro intrusions, and structural features (e.g., detachment faults, normal fault gauges) contribute to the large diversity in alteration types observed. This diversity of peridotite-seawater reaction products may be common in structurally complex settings such as the Mid-Atlantic Ridge 15°N area.

[58] During initial peridotite-seawater interaction at Sites 1270 and 1271 pyroxenes react to produce talc and tremolite, while olivine remains largely fresh. Experimental calibration suggests that these reactions take place at $T > 350$°C where olivine does not react or reacts at a much slower rate than pyroxenes. Rainbow and Logatchev fluid compositions are consistent with these mineral reactions.

[59] In the absence of pyroxenes (in dunites), or at low temperatures, where pyroxenes react very slowly, the fluids do not become enriched in Si and serpentine, magnetite, and brucite form. These reactions are documented in dunites of Site 1271 and dunites and harzburgites of Site 1274 and likely take place at temperatures <250°C. In many oceanic serpentinites, brucite, tremolite, and talc formed during initial serpentinization are not present, because continued fluid-rock interaction leads to changes in fluid pH and silica activity and causes reaction of these phases to serpentine. In addition, brucite dissolves in seawater and is not preserved at or near the seafloor.

[60] If seawater-rock interaction continues after serpentinization is largely completed, oxidizing conditions prevail as indicated by the abundance of hematite in Hole 1268A and iowaite in Hole 1272A. The Ca poor nature of the dunites and depleted harzburgites (in particular after serpentinization is completed) may in part be responsible for the prevalence of oxidizing conditions if the release of Ca to the fluid is insufficient to precipitate seawater sulfate as anhydrite. Local pervasive talc alteration suggests that mass transfer during post-serpentinization reactions can be significant. Talc alteration is not limited to shear zones and pervasive talc alteration under static conditions is common at Site 1268. We suggest that this talc alteration is due to silica metasomatism and that the silica is mobilized from gabbros and harzburgite undergoing high-temperature (>350°C) fluid-rock interactions.

Acknowledgments

[61] The Ocean Drilling Program Leg 209 Shipboard Scientific Party members are Natsue Abe, Wolfgang Bach, Richard Carlson, John Casey, Lynne Chambers, Michael Cheadle, Anna Cipriani, Henry Dick, Ulrich Faul, Miguel Garces, Carlos Garrido, Jeffrey Gee, Marguerite Godard, David Graham, Dale Griffin, Jason Harvey, Benoit Ildefonse, Gerardo Iturrino, Jennifer Josef, Peter Kelemen, Eiichi Kikawa, William Meurer, Jay Miller, Holger Paulick, Martin Rosner, Timothy Schroeder, Monique Seyler, and Eiichi Takazawa (Ocean Drilling Program, Texas A&M University, 1000 Discovery Drive, College Station, TX 77845, USA). We thank the captain and crew of the JOIDES Resolution and the Ocean Drilling Program and staff for making this study possible. This research used data and/or samples supplied by the Ocean Drilling Program (ODP). ODP is sponsored by the U.S. National Science Foundation (NSF) and participating countries under management of Joint Oceanographic Institutions (JOI), Inc. We thank Jeff Seewald and Meg Tivey for useful discussions and Bill Seyfried and Jeff Alt for insightful formal reviews. Funding for this research was provided by JOI/USSAC and NSF-OCE grant 9986135. This is WHOI contribution 11,193.

References

Abrajano, T. A., N. C. Sturchio, J. K. Böhlke, G. L. Lyon, R. J. Poreda, and C. M. Stevens (1988), Methane-hydrogen gas seeps, Zambales Ophiolite, Philippines: Deep or shallow origin?, *Chem. Geol.*, *71*, 211–222.

Agrinier, P., and M. Cannat (1997), Oxygen-isotope constraints on serpentinization processes in ultramafic rocks from the Mid-Atlantic Ridge (23°N), *Proc. Ocean Drill. Program Sci. Results*, *153*, 381–388.

Agrinier, P., R. Hekinian, D. Bideau, and M. Javoy (1995), O and H stable isotope compositions of oceanic crust and upper mantle rocks exposed in the Hess Deep near the Galapagos Triple Junction, *Earth Planet. Sci. Lett.*, *136*, 183–196.

Allen, D. E., and W. E. J. Seyfried (2003), Compositional controls on vent fluids from ultramafic-hosted hydrothermal systems at mid-ocean ridges: An experimental study at 400°C, 500 bars, *Geochim. Cosmochim. Acta*, *67*(8), 1531–1542.

Allen, D. E., and W. E. J. Seyfried (2004), Serpentinization and heat generation: Constraints from Lost City and Rainbow hydrothermal systems, *Geochim. Cosmochim. Acta*, *68*(6), 1347–1354.

Allman, R., and J. D. H. Donnay (1969), About the structure of iowaite, *Am. Mineral.*, *54*, 296–299.

Alt, J. C. (1995), Subseafloor processes in mid-ocean ridge hydrothermal systems, in *Seafloor Hydrothermal Systems: Physical, Chemical, Biological and Geological Interactions*, *Geophys. Monogr. Ser.*, vol. 91, edited by S. E. Humphris et al., pp. 85–114, AGU, Washington, D. C.

Alt, J. C., and W. C. Shanks (1998), Sulfur in serpentinized oceanic peridotites: Serpentinization processes and microbial sulfate reduction, *J. Geophys. Res.*, *103*, 9917–9929.

Alt, J. C., and W. C. Shanks (2003), Serpentinization of abyssal peridotites from the MARK area, Mid-Atlantic Ridge: Sulfur geochemistry and reaction modeling, *Geochim. Cosmochim. Acta*, *67*(4), 641–653.

Aumento, F., and H. Loubat (1971), The Mid-Atlantic Ridge Near 45°N, XVI, Serpentinized ultramafic intrusions, *Can. J. Earth Sci.*, *8*, 631–663.

Bach, W., N. R. Banerjee, H. J. B. Dick, and E. T. Baker (2002), Discovery of ancient and active hydrothermal systems along the ultra-slow spreading Southwest Indian Ridge 10°–16°E, *Geochem. Geophys. Geosyst.*, *3*(7), 1044, doi:10.1029/2001GC000279.

Beard, J. S., and L. Hopkinson (2000), A fossil, serpentinization-related hydrothermal vent, Ocean Drilling Program Leg 173, Site 1068 (Iberia Abyssal Plain): Some aspects of mineral and fluid chemistry, *J. Geophys. Res.*, *105*(B7), 16,527–16,539.

Bideau, D., R. Hebert, R. Hekinian, and M. Cannat (1991), Metamorphism of deep-seated rocks from the Garrett Ultrafast Transform (East Pacific Rise Near 13°25′S), *J. Geophys. Res.*, *96*, 10,079–10,099.

Blusztajn, J., and S. R. Hart (1996), Sr and O isotopic ratios of aragonite veins from Site 895, *Proc. Ocean Drill. Program Sci. Results*, *147*, 311–313.

Bonatti, E., J. R. Lawrence, P. R. Hamlyn, and D. Breger (1980), Aragonite from deep sea ultramafic rocks, *Geochim. Cosmochim. Acta*, *44*, 1207–1215.

Bougault, H., L. Dmitriev, J.-G. Schilling, A. Sobolev, J.-L. Joron, and H. D. Needham (1988), Mantle heterogeneity from trace elements: Mid-Atlantic Ridge triple junction near 14°N, *Earth Planet. Sci. Lett.*, *88*, 27–36.

Bougault, H., J. L. Charlou, Y. Fouquet, H. D. Needham, N. Vaslet, P. Appriou, P. J. Baptiste, P. A. Rona, L. Dmitriev, and S. Silantiev (1993), Fast and slow spreading ridges: Structure and hydrothermal activity, ultramafic topography highs, and CH_4 output, *J. Geophys. Res.*, *98*, 9643–9651.

Cannat, M. (1993), Emplacement of mantle rocks in the seafloor at mid-ocean ridges, *J. Geophys. Res.*, *98*, 4163–4172.

Cannat, M., and J. F. Casey (1995), An ultramafic lift at the Mid-Atlantic Ridge: Successive stages of magmatism in serpentinized peridotites from the 15°N region, in *Mantle and Lower Crust Exposed in Oceanic Ridges and in Ophiolites*, edited by R. L. M. Vissers and A. Nicolas, pp. 5–34, Kluwer Acad., Norwell, Mass.

Cannat, M., D. Bideau, and H. Bougault (1992), Serpentinized peridotites and gabbros in the Mid-Atlantic Ridge axial valley at 15°37 and 16°52, *Earth Planet. Sci. Lett.*, *109*, 87–106.

Cannat, M., Y. Lagabrielle, N. de Coutures, H. Bougault, J. Casey, L. Dmitriev, and Y. Fouquet (1997), Ultramafic and gabbroic exposures at the Mid-Atlantic Ridge: Geological mapping in the 15°N region, *Tectonophysics*, *279*, 193–213.

Casey, J. F., M. G. Braun, and P. K. Kelemen (1998), Megamullions along the Mid-Atlantic Ridge between 14°N and 16°N: Results of Leg 1, JAMSTEC/WHOI MODE 98 Survey, *Eos Trans. AGU*, *79*(45), Fall Meet. Suppl., F920.

Charlou, J.-L., Y. Fouquet, H. Bougault, J. P. Donval, J. Etoubleau, P. Jean-Baptiste, A. Dapoigny, P. Appriou, and P. A. Rona (1998), Intense CH_4 plumes generated by serpentinization of ultramafic rocks at the intersection of the 15°20′N fracture zone and the Mid-Atlantic Ridge, *Geochim. Cosmochim. Acta*, *62*(13), 2323–2333.

Charlou, J.-L., J.-P. Donval, Y. Fouquet, P. Jean-Baptiste, and N. Holm (2002), Geochemistry of high H_2 and CH_4 vent fluids issuing from ultramafic rocks at the Rainbow hydrothermal field (36°14′N, MAR), *Chem. Geol.*, *191*, 345–359.

Craig, J. R. (1973), Pyrite-pentlandite assemblages and other low temperature relations in the Fe-Ni-S system, *Am. J. Sci.*, *273*, 496–510.

Dick, H. J. B., and P. B. Kelemen (1992), Light rare earth element enriched clinopyroxene in harzburgites from 15°05′N on the Mid-Atlantic Ridge, *Eos Trans. AGU*, *73*(43), Fall Meet. Suppl., 584.

Dilek, Y., A. Coulton, and S. D. Hurst (1997), Serpentinization and hydrothermal veining in peridotites at Site 920 in the MARK area, *Proc. Ocean Drill. Program Sci. Results*, *153*, 35–59.

D'Orazio, M., C. Boschi, and D. Brunelli (2004), Talc-rich hydrothermal rocks from the St. Paul and Conrad fracture zones in the Atlantic Ocean, *Eur. J. Mineral.*, *16*, 73–83.

Dosso, L., and H. Bougault (1986), A hot spot at 14°N on the Mid-Atlantic Ridge: Isotopic (Sr, Nd) and trace element data, *Eos Trans. AGU*, *67*(16), Spring Meet. Suppl., 410.

Dosso, L., H. Bougault, and J.-L. Joron (1993), Geochemical morphology of the North Mid-Atlantic Ridge, 10°–24°N: Trace element-isotope complementarity, *Earth Planet. Sci. Lett.*, *120*, 443–462.

Douville, E., J. L. Charlou, E. H. Oelkers, P. Bianvenu, C. F. Jove Colon, J. P. Donval, Y. Fouquet, D. Prieur, and P. Appriou (2002), The rainbow vent fluids (36°14′N, MAR): The influence of ultramafic rocks and phase separation on trace metal contents on Mid-Atlantic Ridge hydrothermal fluids, *Chem. Geol.*, *184*, 37–48.

Eckstrand, O. R. (1975), The Dumont Serpentinite: A model for control of nickeliferous opaque mineral assemblages by alteration reactions in ultramafic rocks, *Econ. Geol.*, *70*, 183–201.

Edmonds, H. N., P. J. Michael, E. T. Baker, D. P. Connelly, J. Snow, C. H. Langmuir, H. J. B. Dick, R. Mühe, C. R. German, and D. W. Graham (2003), Discovery of abundant hydrothermal venting on the ultra-slow spreading Gakkel ridge in the Arctic Ocean, *Nature*, *421*, 252–256.

Escartín, J., and M. Cannat (1999), Ultramafic exposures and the gravity signature of the lithosphere near the Fifteen-Twenty Fracture Zone (Mid-Atlantic Ridge, 14°–16.5°N), *Earth Planet. Sci. Lett.*, *171*, 411–424.

Escartín, J., G. Hirth, and B. Evans (1997), Effects of serpentinization on the lithospheric strength and the style of normal faulting at slow-spreading ridges, *Earth Planet. Sci. Lett.*, *151*, 181–189.

Escartín, J., C. Mével, C. J. MacLeod, and A. M. McCaig (2003), Constraints on deformation conditions and the origin of oceanic detachments: The Mid-Atlantic Ridge core complex at 15°45′N, *Geochem. Geophys. Geosyst.*, *4*(8), 1067, doi:10.1029/2002GC000472.

Evans, B. W. (1977), Metamorphisms of alpine peridotite and serpentinite, *Annu. Rev. Earth Planet. Sci.*, *5*, 398–447.

Frost, B. R. (1985), On the stability of sulfides, oxides and native metals in serpentinite, *J. Petrol.*, *26*, 31–63.

Früh-Green, G. L., A. Plas, and C. Lecuyer (1996), Petrologic and stable isotopic constraints on hydrothermal alteration and serpentinization of the EPR shallow mantle at Hess Deep, Site 895, *Proc. Ocean Drill. Program Sci. Results*, *147*, 109–163.

Früh-Green, G. L., D. S. Kelley, S. M. Bernasconi, J. A. Karson, K. A. Ludwig, D. A. Butterfield, C. Boschi, and G. Proskurowski (2003), 30,000 years of hydrothermal activity at the Lost City vent field, *Science*, *301*, 495–498.

Fujiwara, T., J. Lin, T. Matsumoto, P. B. Kelemen, B. E. Tucholke, and J. F. Casey (2003), Crustal evolution of the Mid-Atlantic Ridge near the Fifteen-Twenty Fracture Zone in the last 5 Ma, *Geochem. Geophys. Geosyst.*, *4*(3), 1024, doi:10.1029/2002GC000364.

German, C. R., E. T. Baker, C. Mevel, K. Tamaki, and F. S. Team (1998), Hydrothermal activity along the southwest Indian ridge, *Nature*, *395*, 490–493.

Gibson, I. L., M. O. Beslier, G. Cornen, K. L. Milliken, and K. E. Seifert (1996), Major and trace element seawater alteration profiles in serpentinite formed during the development of the Iberia margin, Site 897, *Proc. Ocean Drill. Program Sci. Results*, *149*, 519–528.

Hébert, R., A. C. Adamson, and S. C. Komor (1990), Metamorphic petrology of ODP Leg 106/109, Hole 670A, serpentinized peridotites: Serpentinization processes at a slow-spreading ridge environment, *Proc. Ocean Drill. Program Sci. Results*, *106/109*, 103–116.

Helgeson, H. C., J. M. Delany, H. W. Nesbitt, and D. K. Bird (1978), Summary and critique of the thermodynamic properties of rock-forming minerals, *Am. J. Sci.*, *278A*, 1–229.

Heling, D., and A. Schwarz (1992), Iowaite in serpentine muds at Site 778, 779, 780, and 784: A possible cause for the low chlorinity of pore waters, *Proc. Ocean Drill. Program Sci. Results*, *125*, 313–323.

Hemley, J. J., J. W. Montoya, D. R. Shaw, and R. W. Luce (1977), Mineral equilibria in the MgO-SiO2-H2O system-II. Talc-antigorite-forsterite-anthophyllite-enstatite stability relations and some geological applications, *Am. J. Sci.*, *277*, 353–382.

Holm, N. G., and J.-L. Charlou (2001), Initial indications of abiotic formation of hydrocarbons in the Rainbow ultramafic hydrothermal system, Mid-Atlantic Ridge, *Earth Planet. Sci. Lett.*, *191*, 1–8.

Hopkinson, L. J., S. Dee, and C. A. Boulter (2000), Moving reactive interfaces and fractal carbonate replacement patterns in serpentinites: Evidence from the southern Iberia Abyssal Plain, *Mineral. Mag.*, *64*(5), 791–800.

Hopkinson, L., J. S. Beard, and C. A. Boulter (2004), The hydrothermal plumbing of a serpentinite-hosted detachment: Evidence from the West Iberia non-volcanic rifted continental margin, *Mar. Geol.*, *204*, 301–315.

Hostetler, P. B., R. G. Coleman, F. A. Mumpton, and B. W. Evans (1966), Brucite in alpine serpentinites, *Am. Mineral.*, *51*, 75–98.

Janecky, D. R., and W. E. Seyfried Jr. (1986), Hydrothermal serpentinization of peridotite within the oceanic crust: Experimental investigations of mineralogy and major element chemistry, *Geochim. Cosmochim. Acta*, *50*, 1357–1378.

Johnson, J. W., E. H. Oelkers, and H. C. Helgeson (1992), SUPCRT92: A software package for calculating the standard molal thermodynamic properties of minerals, gases, aqueous species, and reactions from 1–5000 bars and 0–1000°C, *Comput. Geosci.*, *18*, 899–947.

Kelley, D. S., and G. L. Früh-Green (1999), Abiogenic methane in deep-seated mid-ocean ridge environments: Insights from stable isotope analyses, *J. Geophys. Res.*, *104*, 10,439–10,460.

Kelley, D. S., and G. L. Früh-Green (2000), Volatiles in mid-ocean ridge environments, in *Ophiolites and Oceanic Crust: New Insights From Field Studies and the Ocean Drilling Program*, edited by Y. Dilek et al., *Spec. Pap. Geol. Soc. Am.*, *349*, 237–260.

Kelley, D. S., et al. (2001), An off-axis hydrothermal vent field near the Mid-Atlantic Ridge at 30 degrees N, *Nature*, *412*, 127–128.

Kohls, D. W., and J. L. Rodda (1967), Iowaite, a new hydrous magnesium hydroxide-ferric oxychloride from the Precambrian of Iowa, *Am. Mineral.*, *52*, 1261–1271.

Krasnov, S. G., et al. (1995), Detailed geological studies of hydrothermal fields in the North Atlantic, in *Hydrothermal*

Vents and Processes, edited by L. M. Parson, C. L. Walker, and D. R. Dixon, *Geol. Soc. Spec. Publ.*, *87*, 43–64.

Martin, B., and W. S. Fyfe (1970), Some experimental and theoretical observations on the kinetics of hydration reactions with particular reference to serpentinization, *Chem. Geol.*, *6*, 185–202.

McCollom, T. M., and J. S. Seewald (2001), A reassessment of the potential for reduction of dissolved CO_2 to hydrocarbons during serpentinization of olivine, *Geochim. Cosmochim. Acta*, *65*, 3769–3778.

Mével, C. (2003), Serpentinization of abyssal peridotite at mid-ocean ridges, *C. R. Geosci.*, *335*, 825–852.

Mével, C., and C. Stadoumi (1996), Hydrothermal alteration of the upper mantle section at Hess Deep, *Proc. Ocean Drill. Program Sci. Results*, *147*, 293–309.

Mével, C., M. Cannat, P. Gente, E. Marion, J. M. Auzende, and J. A. Karson (1991), Emplacement of deep crustal and mantle rocks on the west median valley wall of the MARK area (MAR, 23°N), *Tectonophysics*, *190*, 31–53.

Murowchick, J. B., and H. L. Barnes (1986), Marcasite precipitation from hydrothermal solutions, *Geochim. Cosmochim. Acta*, *50*, 2615–2629.

Neal, C., and G. Stanger (1983), Hydrogen generation from mantle source rocks in Oman, *Earth Planet. Sci. Lett.*, *66*, 315–320.

Nesbitt, H. W., and O. P. Brickner (1978), Low temperature alteration processes affecting ultramafic bodies, *Geochim. Cosmochim. Acta*, *42*, 403–409.

Normand, C., A. E. Williams-Jones, R. F. Martin, and H. Vali (2002), Hydrothermal alteration of olivine in a flow-through autoclave: Nucleation and growth of serpentine phases, *Am. Mineral.*, *87*, 1699–1709.

O'Brien, D., M. Carton, D. Eardly, and J. W. Patching (1998), In situ filtration and preliminary molecular analysis of microbial biomass from the Rainbow hydrothermal plume at 36°15′N on the Mid-Atlantic Ridge, *Earth Planet. Sci. Lett.*, *157*, 223–231.

O'Hanley, D. S. (1996), *Serpentinites: Records of Tectonic and Petrological History*, 277 pp., Oxford Univ. Press, New York.

O'Hanley, D. S., and F. J. Wicks (1995), Conditions of formation of lizardite, chrysotile and antigorite, Cassiar, British Columbia, *Can. Mineral.*, *33*, 753–773.

Palandri, J. L., and M. H. Reed (2004), Geochemical models of metasomatism in ultramafic systems: Serpentinization, rodingitization, and sea floor carbonate chimney precipitation, *Geochim. Cosmochim. Acta*, *68*(5), 1115–1133.

Peabody, C. E., and M. T. Einaudi (1992), Origin of petroleum and mercury in the Culver-Baer cinnabar deposit, Mayacmas Distirct, California, *Econ. Geol.*, *87*, 1078–1103.

Prichard, H. M. (1979), A petrographic study of the process of serpentinization in ophiolites and the ocean crust, *Contrib. Mineral. Petrol.*, *68*, 231–241.

Saccocia, P. J., K. Ding, M. E. Berndt, J. S. Seewald, and W. E. Seyfried (1994), Experimental and theoretical perspectives on crustal alteration at mid-ocean ridges, in *Alteration and Alteration Processes Associated With Ore-Forming Systems*, *Short Course Notes 11*, edited by D. Lentz, pp. 403–431, Geol. Assoc. of Can., St. John's, Newfoundland, Canada.

Sanford, R. F. (1981), Mineralogical and chemical effects of hydration reactions and applications to serpentinization, *Am. Mineral.*, *66*, 290–297.

Schandl, E. S., D. S. O'Hanley, and F. J. Wicks (1989), Rodingites in serpentinized ultramafic rocks of the Abitibi Greenstone belt, Ontario, *Can. Mineral.*, *27*, 579–591.

Schroeder, T., B. John, and B. R. Frost (2002), Geologic implications of seawater circulation through peridotite exposed at slow-spreading ridges, *Geology*, *30*(4), 367–370.

Seyfried, W. E., and W. E. J. Dibble (1980), Sea water - peridotite interaction at 300 degC and 500 bars: Implications for the origin of oceanic serpentinites, *Geochim. Cosmochim. Acta*, *44*, 309–321.

Seyfried, W. E., and K. Ding (1995), Phase equilibria in subseafloor hydrothermal systems: A review of the role of redox, temperature, pH and dissolved Cl on the chemistry of hot spring fluids on mid-ocean ridges, in *Seafloor Hydrothermal Systems: Physical, Chemical, Biological and Geological Interactions*, *Geophys. Monogr. Ser.*, vol. 91, edited by S. E. Humphris et al., pp. 248–272, AGU, Washington, D. C.

Shipboard Scientific Party (2003), Leg 209 Preliminary Report, *Ocean Drill. Program Prelim. Rep.*, *209* [online]. (Available at http://www-odp.tamu.edu/publications/prelim/209_prel/209PREL.PDF)

Simoneit, B. R. T., A. Y. Lein, V. I. Peresypkin, and G. A. Osipov (2004), Composition and origin of hydrothermal petroleum and associated lipids in the sulfide deposits of the Rainbow Field (Mid-Atlantic Ridge at 36°N), *Geochim. Cosmochim. Acta*, *68*(10), 2275–2294.

Snow, J. E., and H. J. B. Dick (1995), Pervasive magnesium loss by marine weathering of peridotite, *Geochim. Cosmochim. Acta*, *59*, 4219–4235.

Sudarikov, S. M., and A. B. Roumiantsev (2000), Structure of hydrothermal plumes at the Logatchev vent field, 14°45′N, Mid-Atlantic Ridge: Evidence from geochemical and geophysical data, *J. Volcanol. Geotherm. Res.*, *101*, 245–252.

Thompson, G., and W. G. Melson (1970), Boron contents of serpentinites and metabasalts in the oceanic crust: Implications for the boron cycle in the oceans, *Earth Planet. Sci. Lett.*, *8*, 61–65.

Toft, P. B., J. Arkani-Hamed, and S. E. Haggerty (1990), The effects of serpentinization on density and magnetic susceptibility: A petrophysical model, *Phys. Earth Planet. Inter.*, *65*, 137–157.

Wenner, D. B., and H. P. Taylor Jr. (1971), Temperatures of serpentinization of ultramafic rocks based on O18/O16 fractionation between coexisting serpentine and magnetite, *Contrib. Mineral. Petrol.*, *32*, 165–185.

Wetzel, L. R., and E. L. Shock (2000), Distinguishing ultramafic- from basalt-hosted submarine hydrothermal systems by comparing calculated vent fluid compositions, *J. Geophys. Res.*, *105*, 8319–8340.

Wicks, F. J. (1984), Deformation histories as recorded by serpentinites, *Can. J. Mineral.*, *22*, 185–204.

Wicks, F. J., and E. J. W. Whittaker (1977), Serpentinite textures and serpentinization, *Can. Mineral.*, *15*, 459–488.

Zolotov, M. Y., and E. L. Shock (2003), Energy for biologic sulfate reduction in a hydrothermally formed ocean on Europa, *J. Geophys. Res.*, *108*(E4), 5022, doi:10.1029/2002JE001966.